Supporting Information

Lysosome-targeted iridium(III) Compounds with pyridine-triphenylamine Schiff base ligands: Syntheses, antitumor application and mechanism

Shujiao Chen, Xicheng Liu*, Xingxing Ge, Qinghui Wang, Yaoqi Xie, Yingying Hao, Ying Zhang, Lei Zhang, Wenjing Shang, Zhe Liu*

Institute of Anticancer Agents Development and Theranostic Application, The Key Laboratory of Life-Organic Analysis and Key Laboratory of Pharmaceutical Intermediates and Analysis of Natural Medicine, School of Chemistry and Chemical Engineering, Qufu Normal University, Qufu 273165, China.

*Corresponding authors, Email: chemlxc@163.com (X. C. Liu); liuzheqd@163.com (Z. Liu)

Supporting Information

Experimental Section

NMR Spectroscopy

^{1}H NMR spectra were acquired in 5 mm NMR tubes at 25°C on Bruker DPX 500 (^{1}H = 500.13 MHz) spectrometers. ^{1}H NMR chemical shifts were internally referenced to $(CHD_2)(CD_3)SO$ (2.50 ppm) for DMSO-d_6, $CHCl_3$ (7.26 ppm) for chloroform-d_1. All data was carried out using XWIN-NMR version 3.6 (Bruker UK Ltd.).

UV-vis Spectroscopy

The UV-vis spectra of these compounds were recorded by TU-1901 UV spectrophotometer with 1 cm path-length quartz cuvettes (3 mL). Spectra were processed using UV Winlab software. Experiments were carried out at 25 °C unless otherwise stated.

Stability Studies

Solutions of **1**-**6** with final concentrations of 1.5 mM in 80% DMSO-d_6/20% phosphate-buffered saline (PBS, pH ≈ 7.2, prepared from D_2O) were prepared by dissolution of the compounds in DMSO-d_6 followed by rapid dilution with D_2O, respectively. ^{1}H NMR spectra were recorded after various time intervals at 37 °C. The test was done by dissolving the **1**-**6** (1.5 mM) in 80% DMSO-d_6, and it was diluted with PBS buffer (pH ≈ 7.2). ^{1}H NMR spectra were recorded after various time intervals at 37 °C.

BSA binding experiments

The titration experiments including UV-vis absorption and fluorescence quenching were performed at constant concentration of BSA. A BSA stock solution was prepared in Tris buffer (5 mM Tris-HCl/10 mM NaCl at pH = 7.2) and stored at 4 ºC. All spectra were recorded after each successive addition of the compounds and incubation at room temperature for 5 min to complete the interaction. In the UV–vis absorption titration experiment, BSA solution (2.5 mL, 1.0×10^{-5} M) was titrated by successive additions of the stock solutions of Ir compound (1.0×10^{-6} M) and the changes in the BSA absorption were recorded after each addition. The fluorescence emission spectra of BSA in the absence and presence of Ir compound was also recorded with excitation at 285 nm. The concentrations of the Ir compound were 0-10.0 μM, and the concentration of BSA was fixed at 10 μM. Synchronous fluorescence spectra of BSA with various concentrations of compounds (0-10.0 μM) were obtained from 240 to 340 nm when $\Delta\lambda$ = 60 nm and from 260 to

360nm when $\Delta\lambda$ = 15 nm.

Reaction with NADH

The reaction of **1-6** (ca. 1 μM) with NADH (ca. 100 μM) in 20% MeOH/80% H_2O (*v/v*) was monitored by UV-vis at 25 °C after various time intervals. TON was calculated from the difference in NADH concentration after 8 h divided by the concentration of iridium catalyst. The concentration of NADH was obtained using the extinction coefficient ε_{339} = 6220 $M^{-1}cm^{-1}$.

Cell Culture

Both human cancer cells (cervical carcinoma HeLa cells and lung cancer A549 cells) were obtained from Shanghai Institute of Biochemistry and Cell Biology (SIBCB) and were grown in Dubelco's Modified Eagle Medium (DMEM). All media were supplemented with 10% fetal bovine serum, and 1% penicillin-streptomycin solution. All cells were grown at 37 °C in a humidified incubator under 5% CO_2 atmosphere.

Viability assay (MTT assay)

After plating 5000 cells per well in 96-well plates, the cells were preincubated in drug-free media at 37 °C for 24 h before adding different concentrations of the compounds to be tested. In order to prepare the stock solution of the drug, the solid compound was dissolved in DMSO. This stock was further diluted using cell culture medium until working concentrations were achieved. The drug exposure period was 24 h. Subsequently, 15 μL of 5 mg mL^{-1} MTT solution was added to form a purple formazan. Afterwards, 100 μL of dimethyl sulfoxide (DMSO) was transferred into each well to dissolve the purple formazan, and results were measured using a microplate reader (DNM-9606, Perlong Medical, Beijing, China) at an absorbance of 570 nm. Each well was triplicated and each experiment repeated at least three times. IC_{50} values quoted are mean ± SEM.

ROS Determination

Flow cytometry analysis of ROS generation in A549 cells caused by exposure to iridium compounds were carried out using the Reactive Oxygen Species Assay Kit (Beyotime Institute of Biotechnology, Shanghai, China) according to the supplier's instructions. Briefly, 1.5 × 10^6 A549 cancer cells per well were seeded in a six-well plate. Cells were preincubated in drug-free media at 37 °C for 24 h in a 5% CO_2 humidified atmosphere, and then drugs were added at concentrations of 0.25 × IC_{50} and 0.5× IC_{50}. After 24 h of drug exposure, cells were washed twice with PBS and then incubated with the DCFH-DA probe (10 μM) at 37 °C for 30 min, and then

washed triple immediately with PBS. The fluorescence intensity was analyzed by flow cytometry (ACEA NovoCyte, Hangzhou, China). Data were processed using NovoExpress™ software.

Cell Cycle Analysis

The A549 cancer cells at 1.5×10^6 per well were seeded in a six-well plate. Cells were preincubated in drug-free media at 37 °C for 24 h, after which **1** and **6** were added at concentrations of $0.25 \times IC_{50}$, $0.5 \times IC_{50}$, $1.0 \times IC_{50}$ and $2.0 \times IC_{50}$ of **1** and **6** against A549 cancer cells. After 24 h of drug exposure, supernatants were removed by suction and cells were washed with PBS. Finally, cells were harvested using trypsin-EDTA and fixed for 24 h using cold 70% ethanol. DNA staining was achieved by suspending the cell pellets in PBS containing propidium iodide (PI) and RNAse. Cell pellets were washed and suspended in PBS before being analyzed in a flow cytometer (ACEA NovoCyte, Hangzhou, China) using excitation of DNA-bound PI at 488 nm, with emission at 585 nm. Data were processed using NovoExpress™ software. The cell cycle distribution is shown as the percentage of cells containing G_0/G_1, S and G_2/M DNA as identified by propidium iodide staining.

Induction of Apoptosis

Flow cytometry analysis of apoptotic populations of the cells caused by exposure to iridium compounds were carried out using the Annexin V-FITC Apoptosis Detection Kit (Beyotime Institute of Biotechnology, China) according to the supplier's instructions. Briefly, A549 cancer cells (1.5×10^6 / 2 mL per well) were seeded in a six-well plate. Cells were preincubated in drug-free media at 37 °C for 24 h, after which **1** and **6** was added at concentrations of $0.25 \times IC_{50}$, $0.5 \times IC_{50}$, $1.0 \times IC_{50}$, $2.0 \times IC_{50}$ and $3.0 \times IC_{50}$ of **1** and **6** against A549 cancer cells. After 24 h of drug exposure, cells were collected, washed once with PBS, and suspended in 195 μL of annexin V-FITC binding buffer which was then added to 5 μL of annexin V-FITC and 10 μL of PI, and then incubated at room temperature in the dark for 15 min. Subsequently, the buffer placed in an ice bath in the dark. The samples were analyzed by a flow cytometer (ACEA NovoCyte, Hangzhou, China).

Mitochondrial Membrane Assay

Analysis of the changes of mitochondrial potential in cells after exposure to iridium compounds was carried out using the mitochondrial membrane potential assay kit with JC-1 (Beyotime Institute of Biotechnology, Shanghai, China) according to the manufacturer's

instructions. Briefly, 1.5×10^6 A549 cancer cells were seeded in six-well plates left to incubate for 24 h in drug-free medium at 37 °C in a humidified atmosphere. Drug solutions, with the concentration changed from 0. 5 × IC_{50} to 2.0 × IC_{50} of **1** and **6** against A549 cancer cells, were added in triplicate, and the cells were left to incubate for a further 24 h under similar conditions. Supernatants were removed by suction, and each well was washed with PBS before detaching the cells using trypsin-EDTA. Staining of the samples was done in flow cytometry tubes protected from light, incubating for 30 min at ambient temperature. The samples were immediately analyzed by a flow cytometer (ACEA NovoCyte, Hangzhou, China). For positive controls, the cells were exposed to carbonyl cyanide 3-chlorophenylhydrazone, CCCP (5 μM), for 20 min. Data were processed using NovoExpress™ software.

Cellular localization assay

Two Photon Laser Scanning Microscope (*/LSM/880NLO) is produced at Carl Zeiss AG, Germany. LTDR (Life Technologies, USA), MTDR (Life Technologies, USA), CCCP (Sigma Aldrich, USA), chloroquine (Sigma Aldrich, USA) were used as received. A549 cells were seeded into 35 mm dishes (Greiner, Germany) for confocal microscopy. After cultured overnight, the cells were incubated with **1-6** (1.0 × IC_{50}) for 1 h. The treated cells were observed immediately under a confocal microscope with excitation at 488 nm. For colocalization studies, the cells were incubated with compounds (1.0 × IC_{50}) for 1 h. Subsequently, the medium was replaced with staining medium containing MTDR/LDTR and stained for another 20 min and 1 h. The cells were washed twice with PBS, and then viewed immediately under a confocal microscope. Investigation of drug entry pattern: Cells were incubated with compounds (1.0 × IC_{50}) for 1 h, after which media was replaced with staining medium containing CCCP (10 μM, 1 h) chloroquine (50 μM, 1 h) and re-stained for 15 min. The cells were washed twice with PBS, and then viewed immediately under a confocal microscope.

Lysosomal damage assay

A549 cells seeded into six-well plate (Corning) were exposed to **1** and **6** at the indicated concentrations for 12 h. The cells were then washed twice with PBS and incubated with AO (5 μM) at 37 ˚C for 15 min. The cells were washed twice with PBS and visualized by confocal microscopy (LSM/880NLO). Emission was collected at 510 ± 20 nm (green) and 625 ± 20 nm (red) upon excitation at 488 nm.

Experimental

Synthesis of [(η^5-C_5Me_5)$IrCl_2$]$_2$ ***(Dimer1)*** *and [(η^5-$C_5Me_4C_6H_5$)$IrCl_2$]$_2$* ***(Dimer2)***.

$IrCl_3 \cdot 3H_2O$ (0.50 g, 1.7 mmol) was dissolved in MeOH (20 mL) in a microwave vial, pentamethyl cyclopentadiene (0.69 g, 5.0 mmol) was added and reacted at 127 °C, 400 psi for 30 min in a microwave instrument. The reaction mixture was allowed to cool to ambient temperature and the dark green precipitate was filtered off. The volume of the dark red filtrate was reduced to ca. 15 mL on a rotary evaporator. Upon cooling to ambient temperature, an orange precipitate appeared and was collected by filtration. The product was washed with methanol and diethyl ether, dried in air, and pure **Dimer 1** was obtained. Yield: 0.40 g (65%). ^{1}H NMR (500 MHz, $CDCl_3$): δ 1.60 (s, J = 1.4 Hz, 15H, C_5Me_5-*H*).

Dimer 2 was synthesized using phenyltetramethyl cyclopentadiene (0.84 g, 5.0 mmol) and $IrCl_3 \cdot 3H_2O$ (0.50 g, 1.67 mmol) according to the method of **Dimer 1**. Yield: 0.37 g (58.5%). ^{1}H NMR (500 MHz, $CDCl_3$): δ 7.58 (m, 2H, Ar-*H*), 7.35 (m, 3H, Ar-*H*), 1.72 (s, 6H, $C_5Me_4C_6H_5$-CH_3), 1.63 (s, 6H, $C_5Me_4C_6H_5$-CH_3)

*Synthesis of [(η^5-C_5Me_5)Ir(biPy)Cl] (**7**) and [(η^5-$C_5Me_4C_6H_5$)Ir(biPy)Cl] (**8**)*

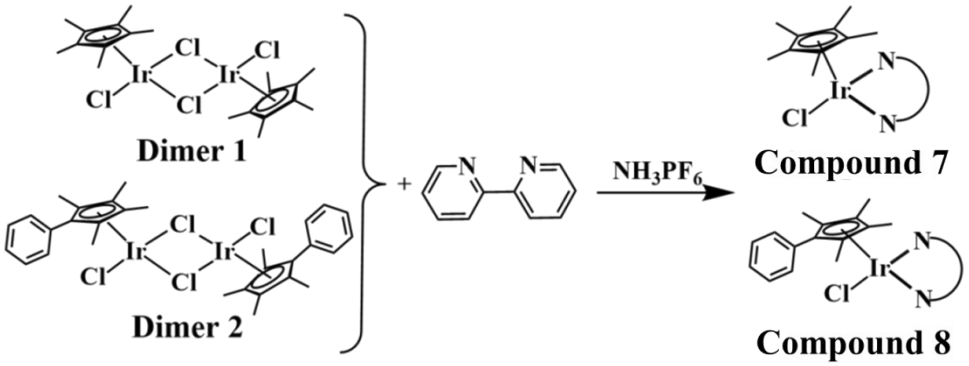

Scheme S1. Design strategy of **7** and **8**.

The general process is as follows: Dimer of iridium (**1** and **2**, 0.05mmol), bipyridine (15.6 mg, 0.1mmol) and ammonium hexafluorophosphate (97.8 mg, 0.6 mmol) were added to 40 mL of Methanol and stired at ambient temperature overnight under N_2 atmosphere. The solvent was removed under reduced pressure, and added 20 mL dichloromethane, the precipitate (sodium acetate) was removed by filtration. Most of the solvent is concentrated to 2.0 mL in vacuum and kept at -20 °C for 12 h, filtered and washed with cold methanol and diethyl ether. The ^{1}H NMR and ESI-MS are shown in Scheme S1. The data were listed as follows:

[(η^5-C_5Me_5)Ir(biPy)Cl] (**7**): Yield:83.6%. ^{1}H NMR (500 MHz, DMSO) δ 8.99 (d, *J* = 5.2 Hz, 2H, Ar-*H*), 8.79 (s, 1H, Ar-*H*), 8.78 (s, 1H, Ar-*H*), 8.34 (td, *J* = 8.0, 1.3 Hz, 2H, Ar-*H*), 7.88 – 7.85 (m, 2H, Ar-*H*), 1.67 (s, 15H, C_5Me_5-*H*). ^{13}C NMR (126 MHz, DMSO) δ 155.37, 152.50, 140.84, 129.45, 124.58, 89.59, 8.57 (C_5Me_5-*C*H_3). ESI-MS (*m/z*): Calcd for $C_{20}H_{23}ClF_6IrN_2P$: $[M\text{-}PF_6]^+$, 519.1; Found 519.1.

[(η^5-$C_5Me_4C_6H_5$)Ir(biPy)Cl] (**8**):Yield: 76.5%.^{1}H NMR (500 MHz, DMSO) δ 8.83 (d, *J* = 8.1 Hz, 2H, Ar-*H*), 8.70 (d, *J* = 5.4 Hz, 2H, Ar-*H*), 8.35 (t, *J* = 7.8 Hz, 2H, Ar-*H*), 7.81 (t, *J* = 6.6 Hz, 2H, Ar-*H*), 7.50 (t, *J* = 5.7 Hz, 5H, Ar-*H*), 1.77 (s, 6H, $C_5Me_4C_6H_5$-C*H*$_3$), 1.68 (s, 6H, $C_5Me_4C_6H_5$-*CH*$_3$). ^{13}C NMR (126 MHz, DMSO) δ 155.55, 151.83, 141.10, 130.43, 129.88, 129.79, 129.51, 129.21, 124.89, 98.66, 87.52, 82.63, 9.67 ($C_5Me_4C_6H_5$-*C*H_3), 8.50 ($C_5Me_4C_6H_5$-*C*H_3). ESI-MS (*m/z*): Calcd for $C_{25}H_{25}ClF_6IrN_2P$: $[M\text{-}PF_6]^+$, 581.1; Found 581.2.

Figures

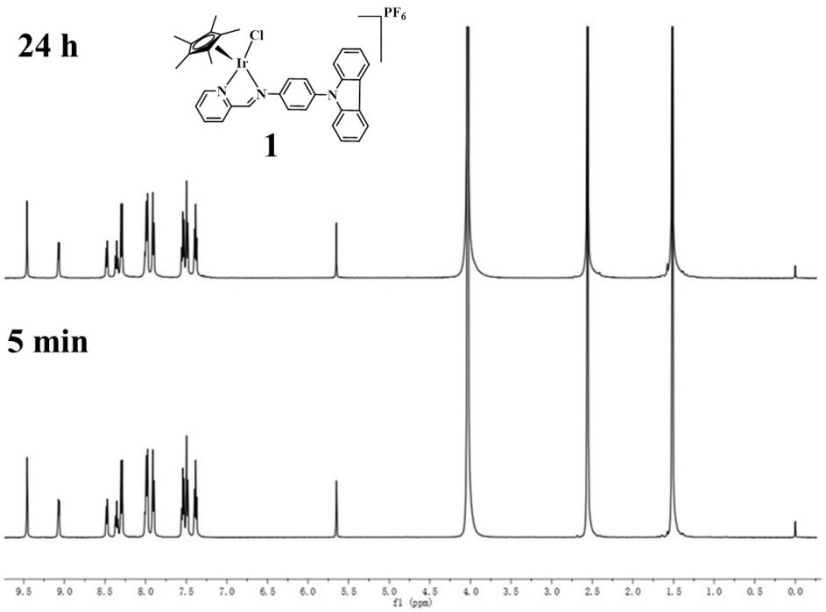

Figure S1. ^{1}H NMR spectra showing the stability of **1** (1.5 mM) in 80% DMSO-d_6/20% PBS (*v*/*v*) at 37 °C. (PBS : pH ≈ 7.2, PBS is prepared from D_2O)

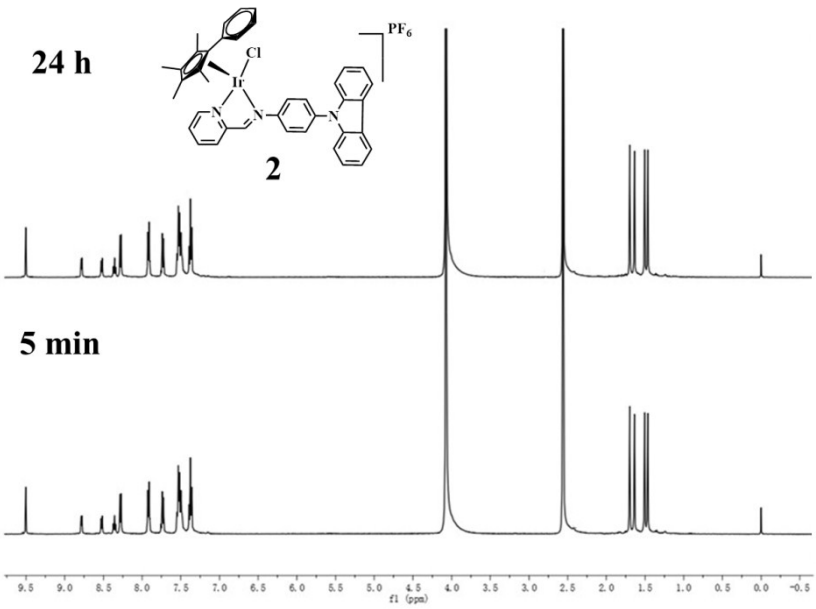

Figure S2. ^{1}H NMR spectra showing the stability of **2** (1.5 mM) in 80% DMSO-d_6/20% PBS (*v*/*v*) at 37 °C. (PBS : pH ≈ 7.2, PBS is prepared from D_2O)

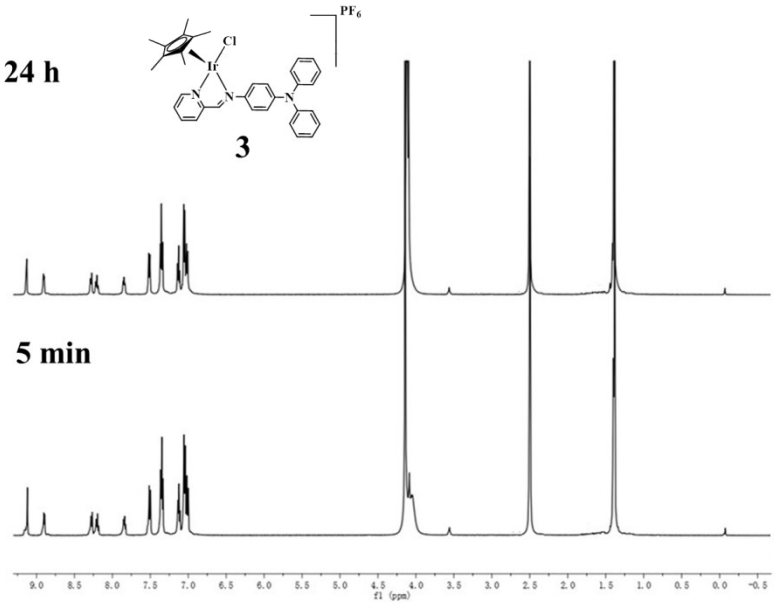

Figure S3. ^{1}H NMR spectra showing the stability of **3** (1.5 mM) in 80% DMSO-d_6/20% PBS (*v*/*v*) at 37 °C. (PBS : pH ≈ 7.2, PBS is prepared from D_2O)

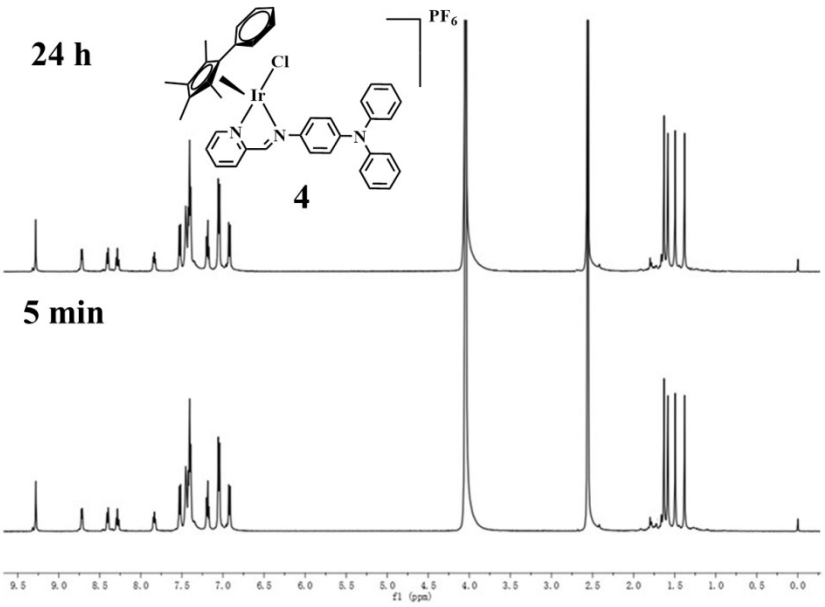

Figure S4. ^{1}H NMR spectra showing the stability of **4** (1.5 mM) in 80% DMSO-d_6/20% PBS (*v*/*v*) at 37 °C. (PBS : pH ≈ 7.2, PBS is prepared from D_2O)

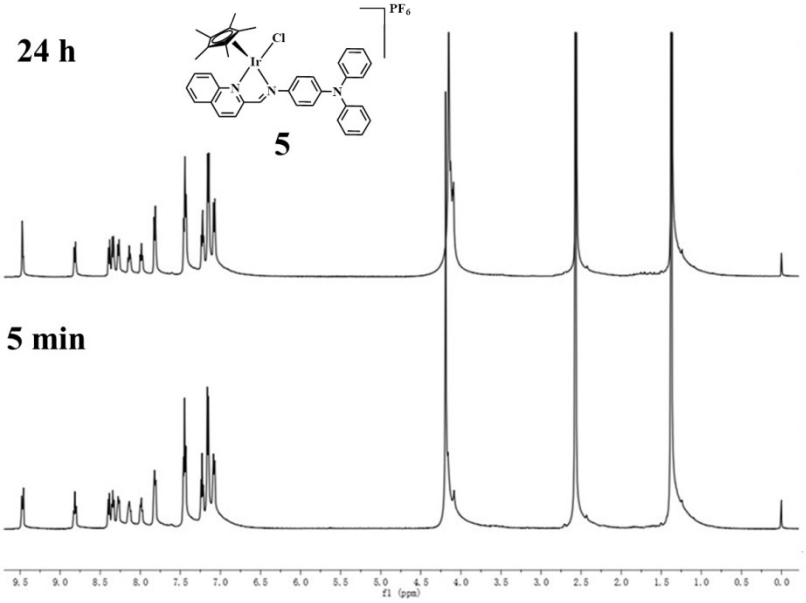

Figure S5. ^{1}H NMR spectra showing the stability of **5** (1.5 mM) in 80% DMSO-d_6/20% PBS (*v*/*v*) at 37 °C. (PBS : pH ≈ 7.2, PBS is prepared from D_2O)

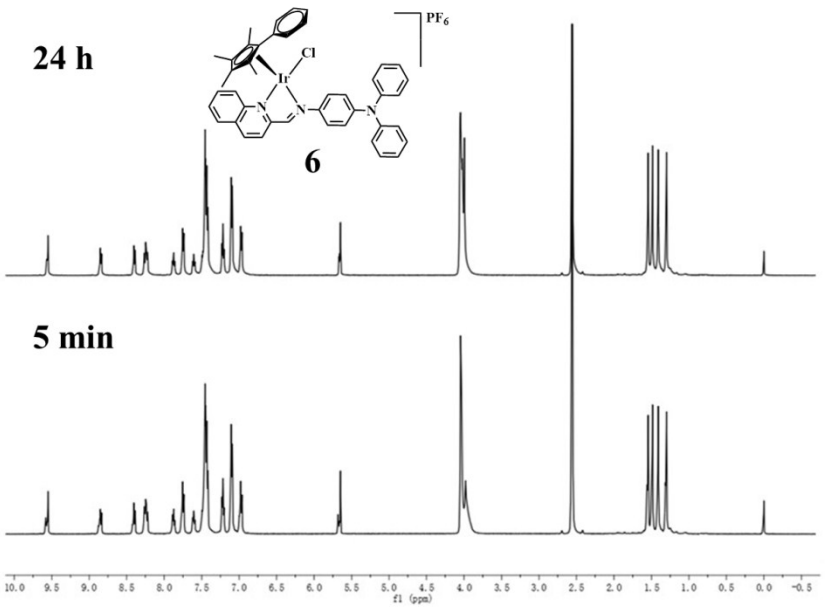

Figure S6. ^{1}H NMR spectra showing the stability of **6** (1.5 mM) in 80% DMSO-d_6/20% PBS (*v*/*v*) at 37 °C. (PBS : pH ≈ 7.2, PBS is prepared from D_2O)

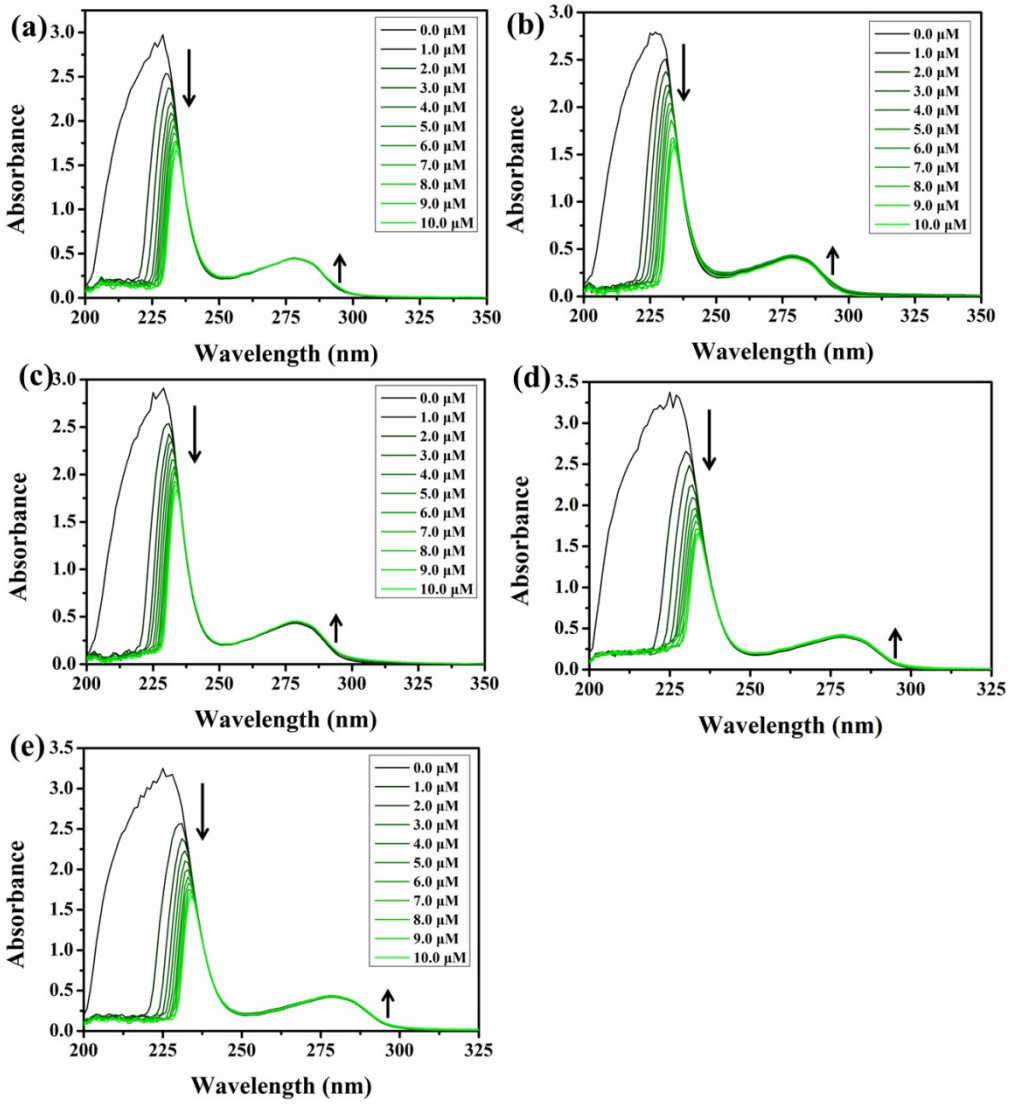

Figure S7. UV-vis spectrum of BSA (10.0 μM) in 5 mM Tris-HCl/10 mM NaCl buffer solution (pH: 7.2) upon addition of the **1** (a), **2** (b),**3** (c), **4** (d) and **5**(e) (0.0-10.0 μM).

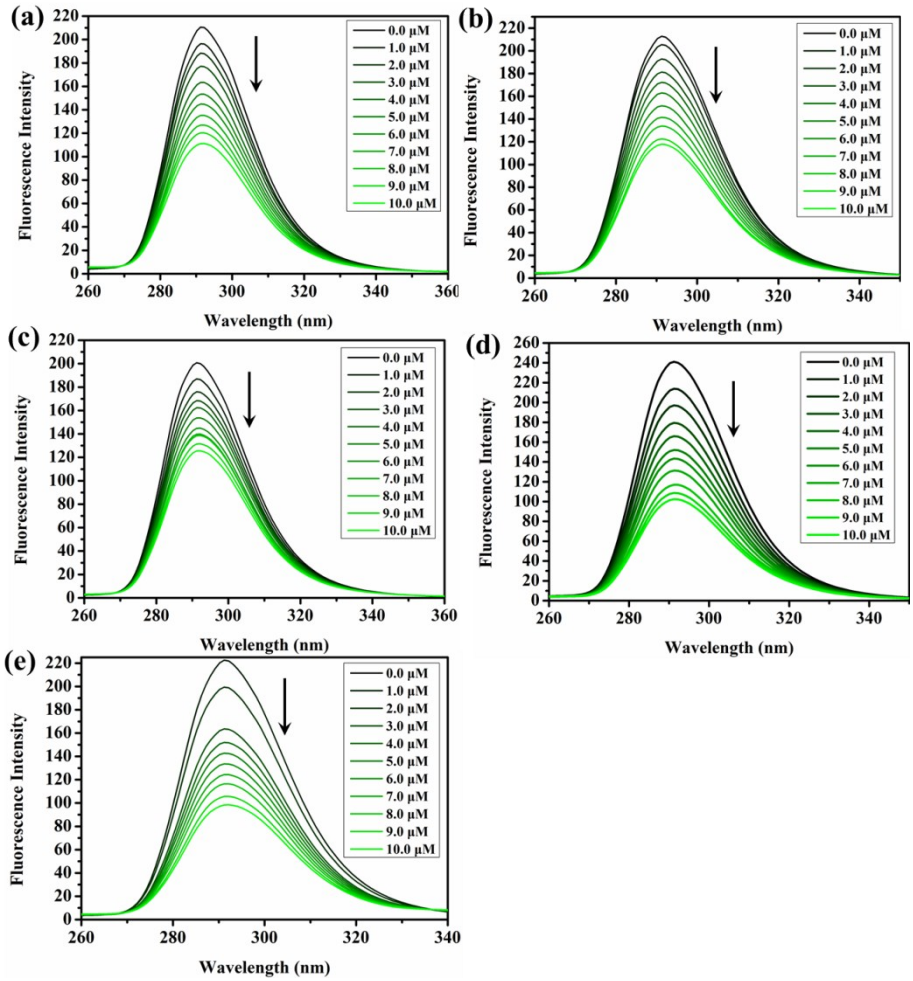

Figure S8. Synchronous spectra of BSA (10.0 μM, 50.0 mM Tris-HCl, 50.0 mM NaCl, pH = 7.2) in the presence of increasing amounts of **1**- **5** (0.0-10.0 μM) with a wavelength difference of $\Delta\lambda$ = 15 nm for **1** (a), **2** (b), **3** (c), **4** (d) and **5** (e).

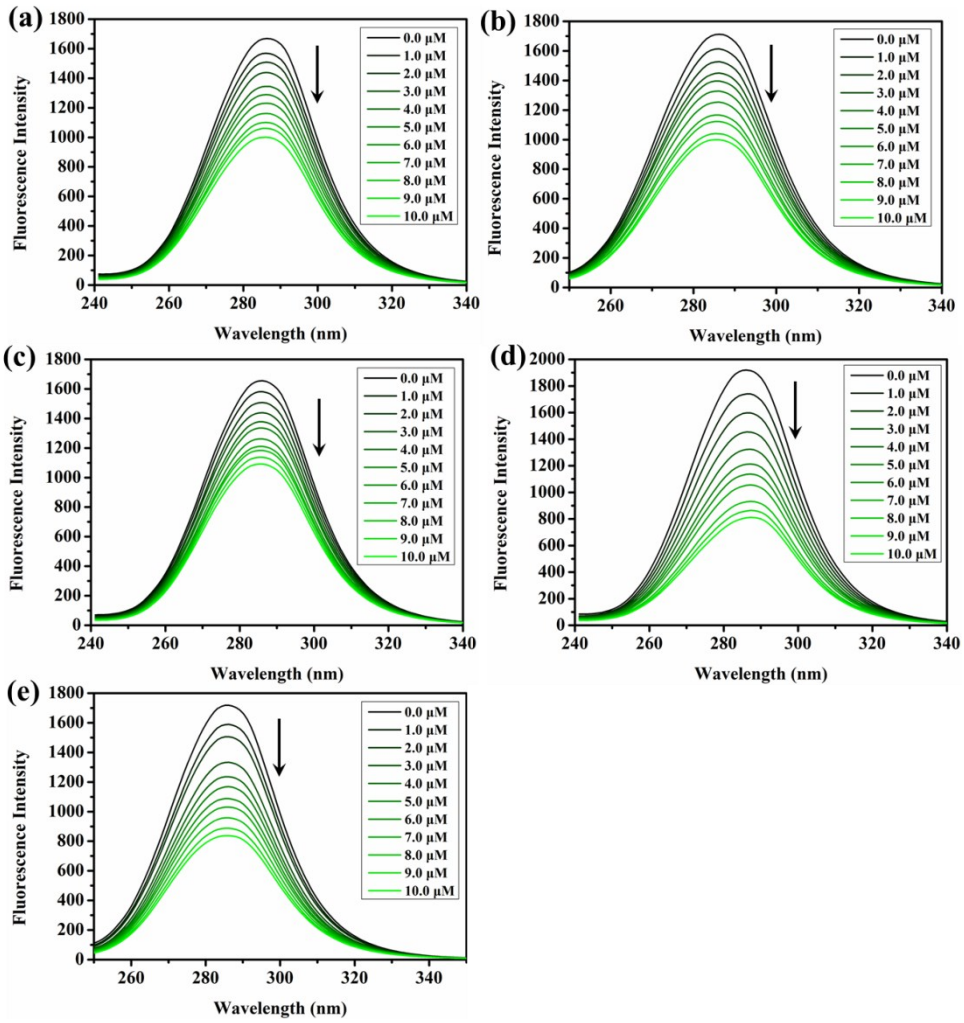

Figure S9. Synchronous spectra of BSA (10.0 μM, 50.0 mM Tris-HCl, 50.0 mM NaCl, pH = 7.2) in the presence of increasing amounts of **1**- **5** (0.0-10.0 μM) with a wavelength difference of $\Delta\lambda$ = 60 nm for **1** (a), **2** (b), **3** (c), **4** (d) and **5** (e).

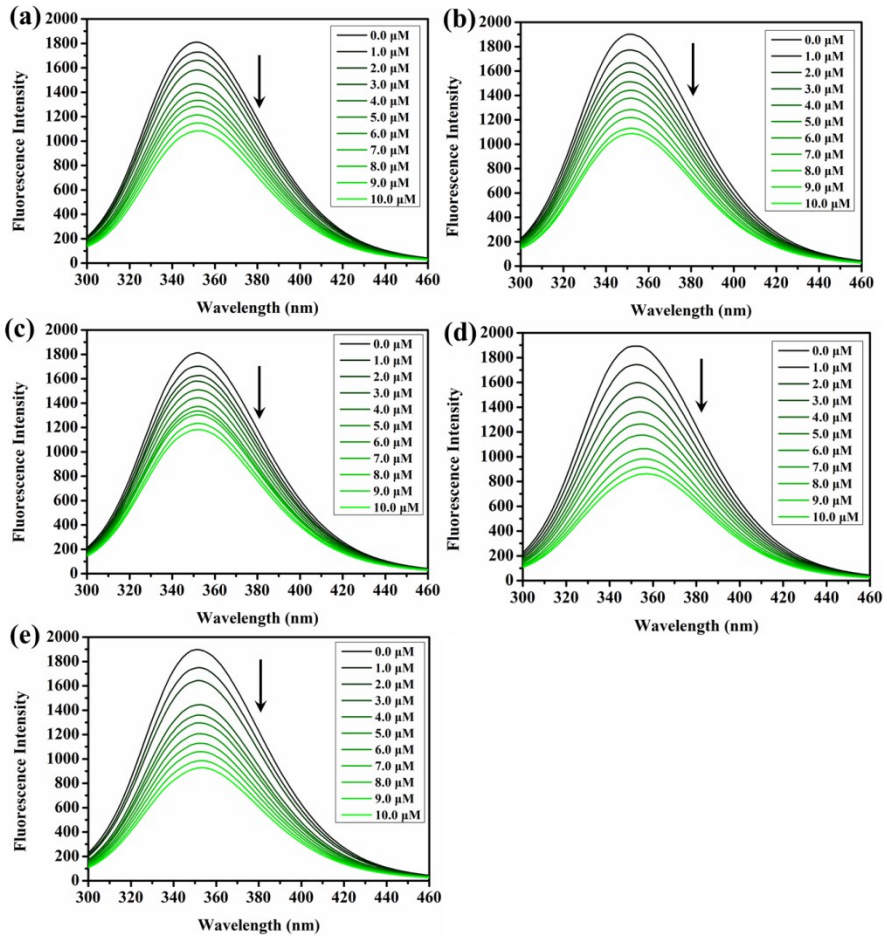

Figure S10. Fluorescence spectra of BSA (10.0 μM; λex = 280 nm; λem = 350 nm) in the absence and presence of the **1** (a), **2** (b), **3** (c), **4** (d) and **5** (e) (0-10.0 μM). The arrow shows the intensity changes in increasing concentration of the Ir(III) compound.

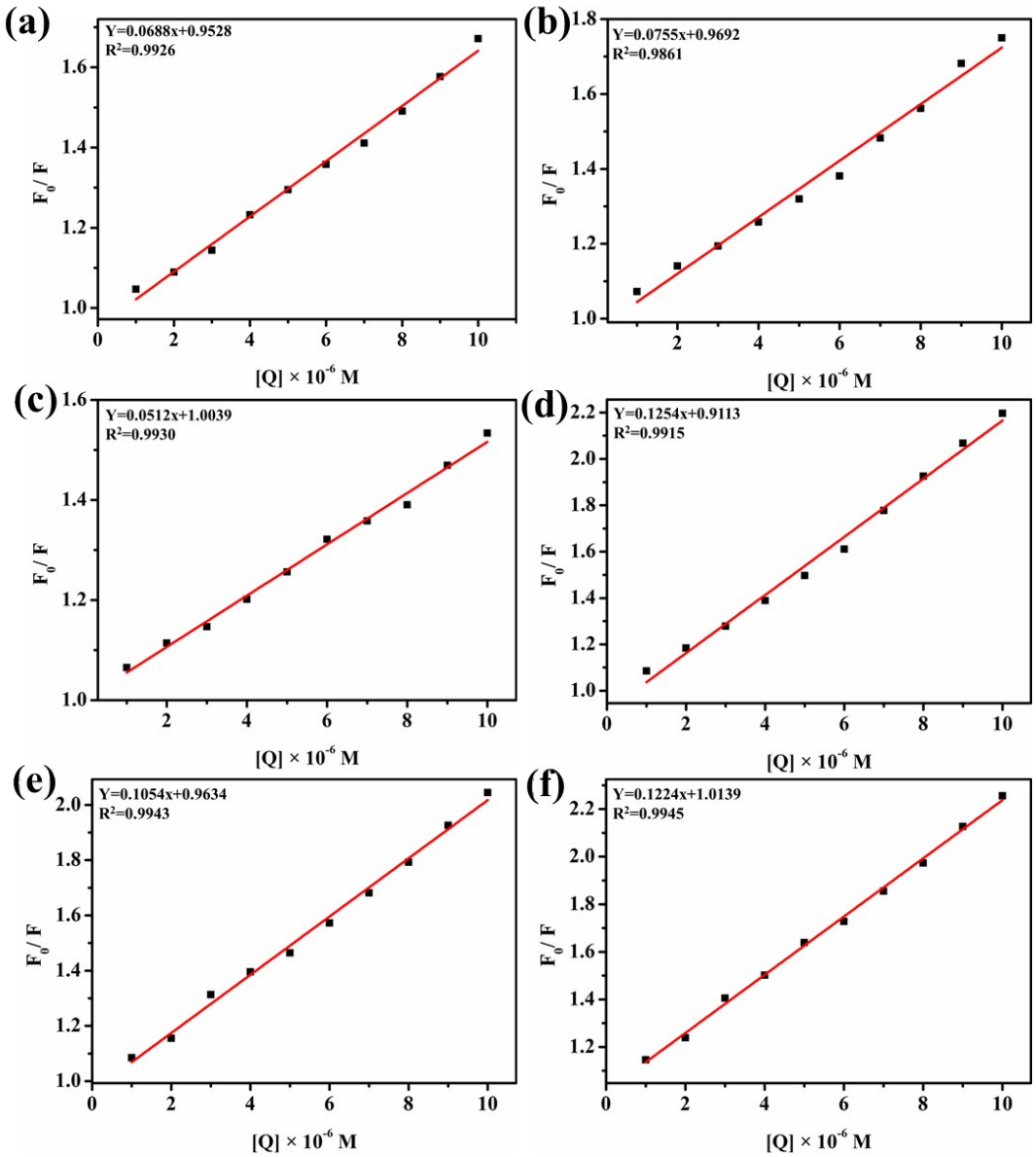

Figure S11. Stern – Volmer plots of F_0/F against the concentration of **1** (a), **2** (b), **3** (c), **4** (d), **5** (e) and **6** (f) (0-10.0 μM).

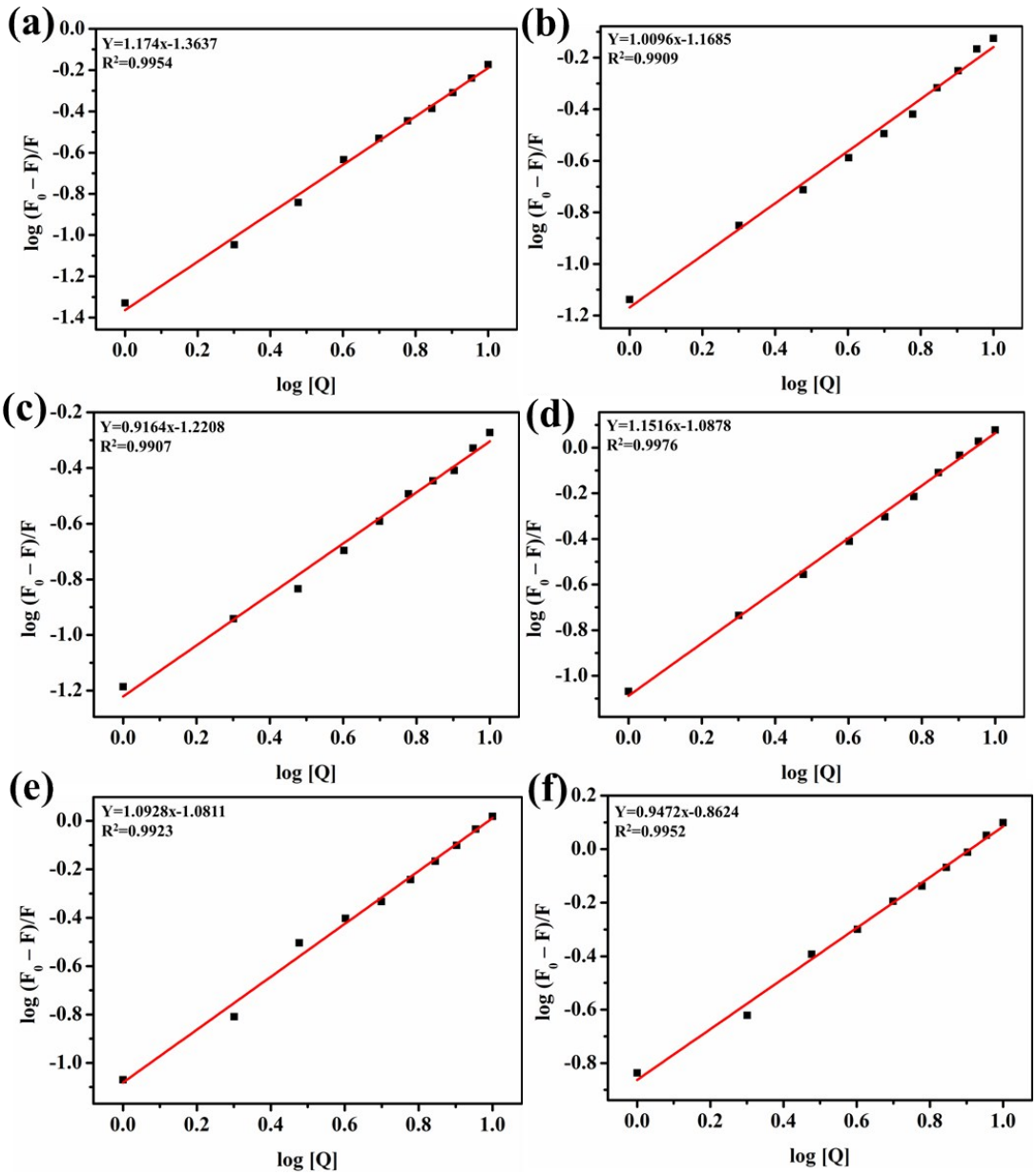

Figure S12. Plots of log [(F_0- F)/F] vs log [Q] for the interaction of BSA with **1** (a), **2** (b), **3** (c), **4** (d), **5** (e) and **6** (f) (0-10.0 μM).

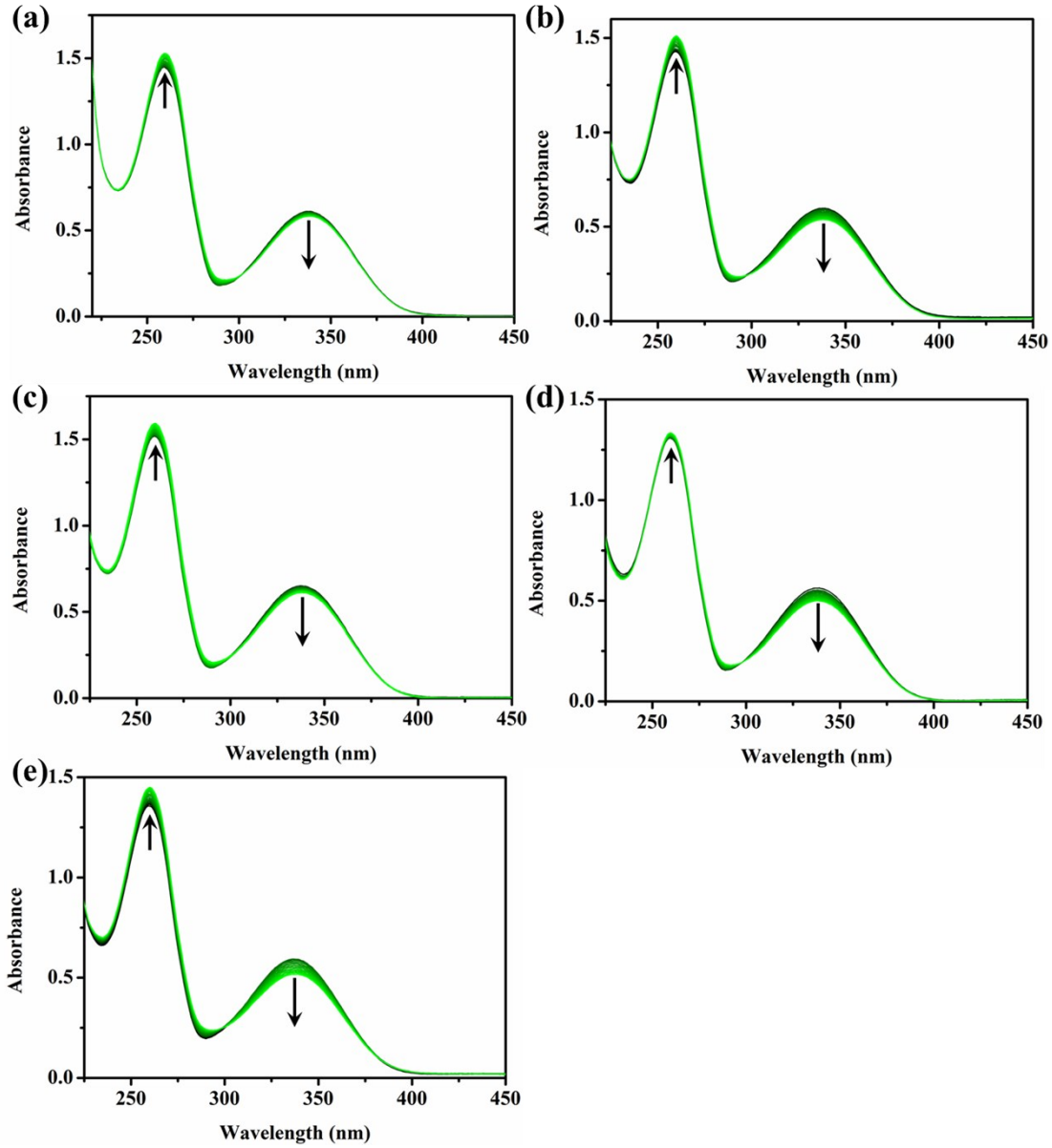

Figure S13. UV-vis spectra of the reaction of NADH (100.0 μM) with **(**a**) 1**, **(**b**) 2**, (c) **3**, **(**d**) 4** and **(**e**) 5** (1.0 μM) in 20% MeOH/80% H_2O (*v:v*) at 25 °C for 8 h.

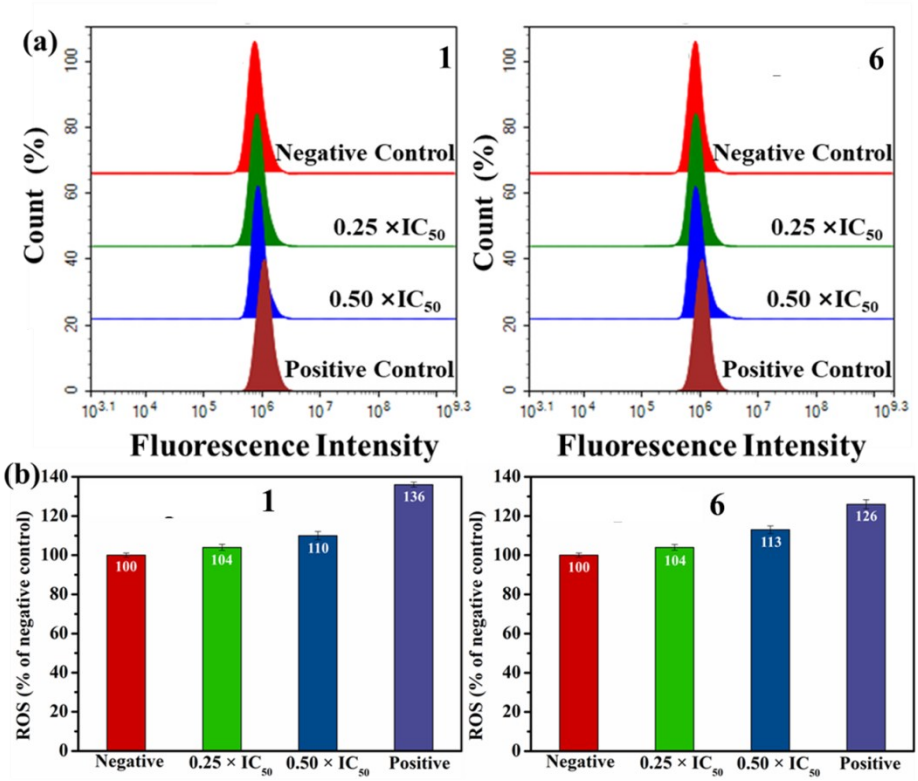

Figure S14. (a) ROS induction in A549 cells treated with **1** and **6** at the 0.25 × IC_{50} and 0.5 × IC_{50} for 24 h. (b) Histograms of ROS levels. Data are quoted as mean ± SD of three replicates.

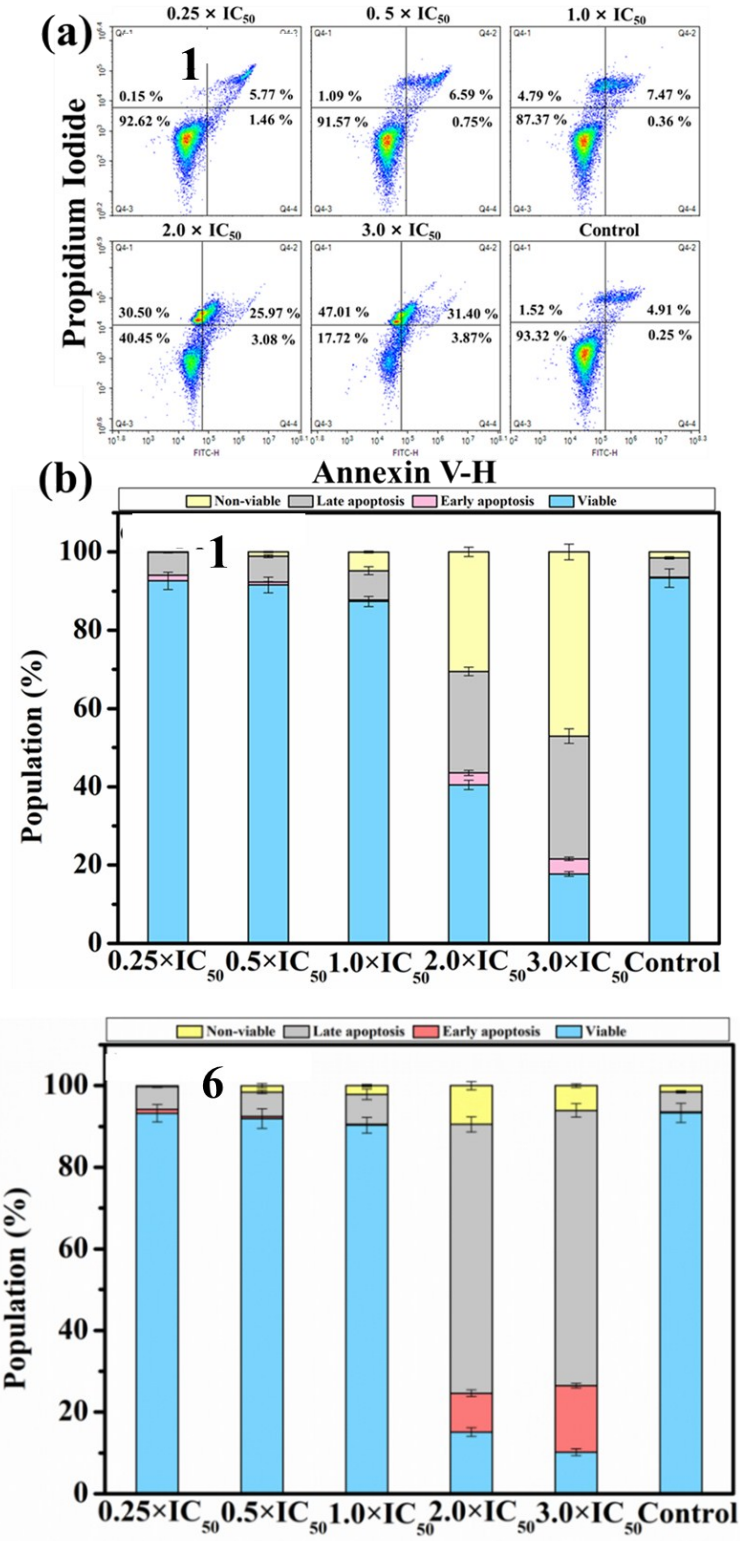

Figure S15. (a) Apoptosis analysis of A549 cells after exposure to **1** for 24 h at 37 °C and determined by flow cytometry using Annexin VFITC/PI staining. (b) Histograms of apoptosis assay. Data are quoted as mean ± SD of three replicates.

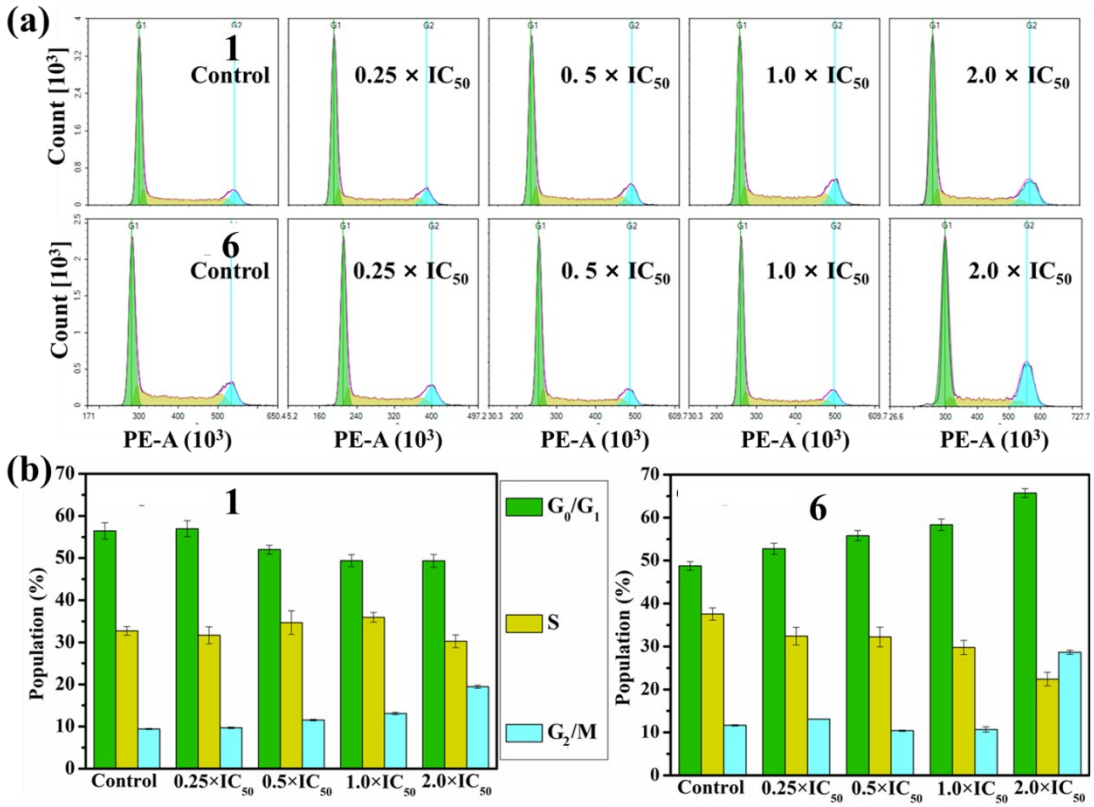

Figure S16. (a) Flow cytometry data for cell cycle distribution of A549 cancer cells exposed to **1** and **6** for 24 h. Concentrations used were 0.25 × IC_{50}, 0.5 × IC_{50}, 1.0 × IC_{50} and 2.0 × IC_{50} Cell staining for flow cytometry was carried out using PI/RNase. Cell populations in each cell cycle phase for control. (b) Histogram of Flow cytometry data for cell cycle distribution of A549 cancer cells exposed to **1** and **6** for 24 h. Data are quoted as mean ± SD of three replicates.

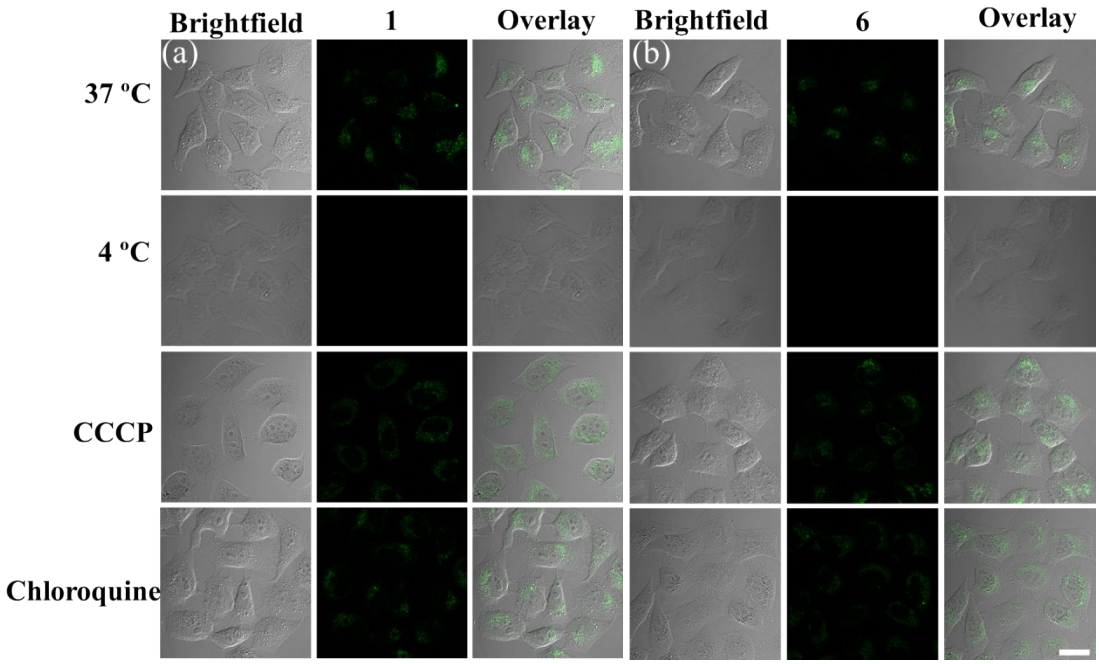

Figure S17. Confocal images of A549 cells after incubation with (a) **1** and (b) **6** (1.0 × IC_{50}) under different conditions. Control cells without inhibitor at 37 °C; 4 °C; addition of CCCP (10 μM) at 37 °C; addition of

chloroquine (50.0 μM) at 37 °C. **1** was excited at 488 nm and emission was collected at 550 ± 30 nm. Scale bar: 20 μm.

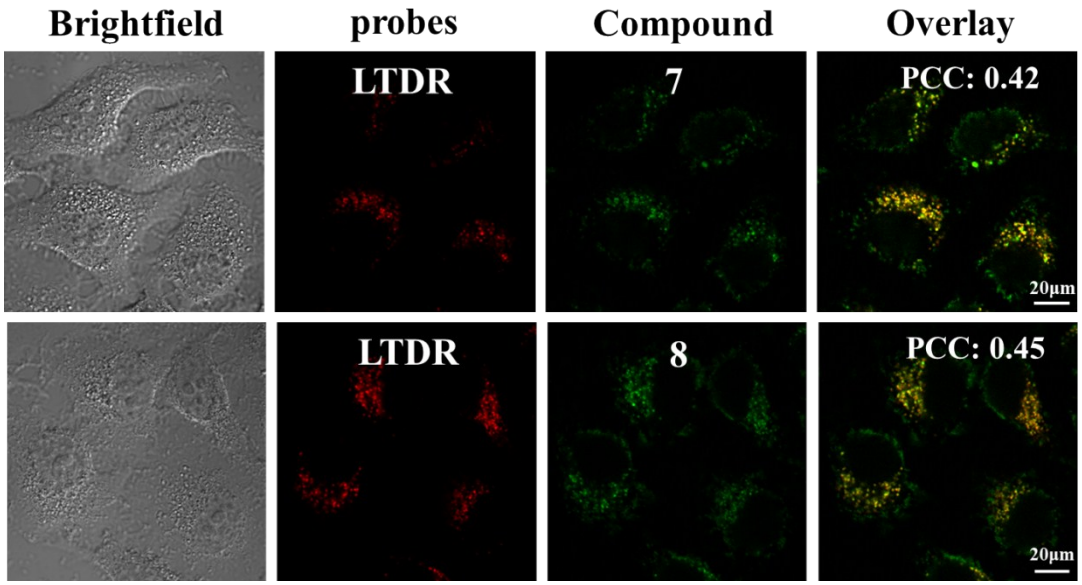

Figure S18. The intercellular localization of **7** and **8** were determined by confocal microscopy. A549 cells were incubated with **7** or **8** (10.0 μM) for 1 h at 37 °C, then incubated with LTDR (75 nM) for 20 min. Compounds were excited at 488 nm and collected at 550 ± 30 nm. LTDR was excited at 594 nm and collected at 630 ± 30 nm.

^{1}HNMR Spectra

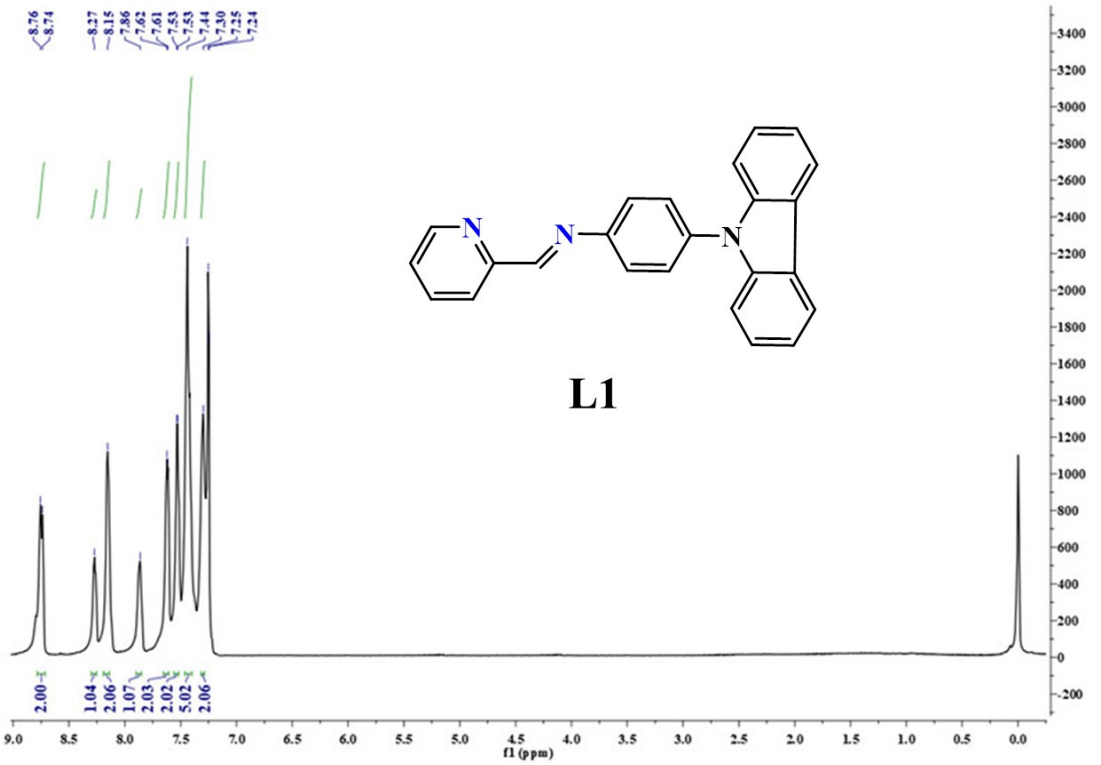
8.76
8.74
8.27
8.15
7.86
7.62
7.61
7.53
7.53
7.44
7.30
7.25
7.24
2.00
1.04
2.06
1.07
2.03
2.02
5.02
2.06
f1 (ppm)

L1

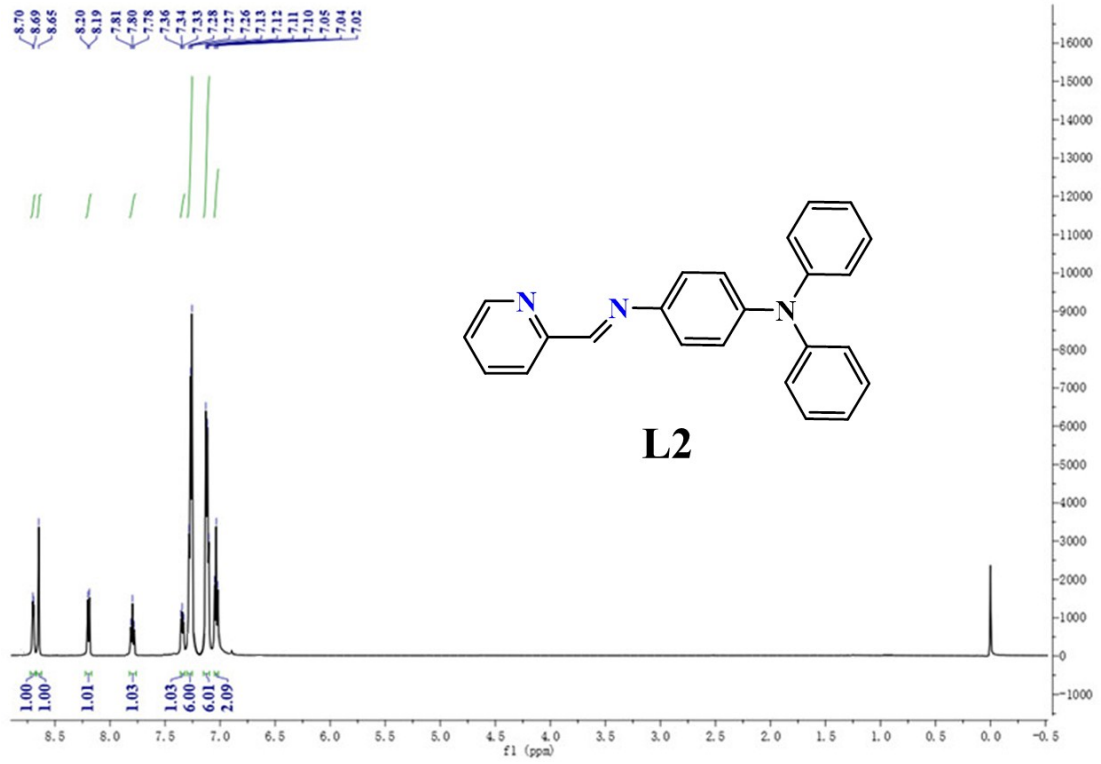
8.70
8.69
8.65
8.20
8.19
7.81
7.80
7.78
7.36
7.34
7.33
7.28
7.27
7.26
7.13
7.12
7.11
7.10
7.05
7.04
7.02
1.00
1.00
1.01
1.03
1.03
6.00
6.01
2.09
f1 (ppm)

L2

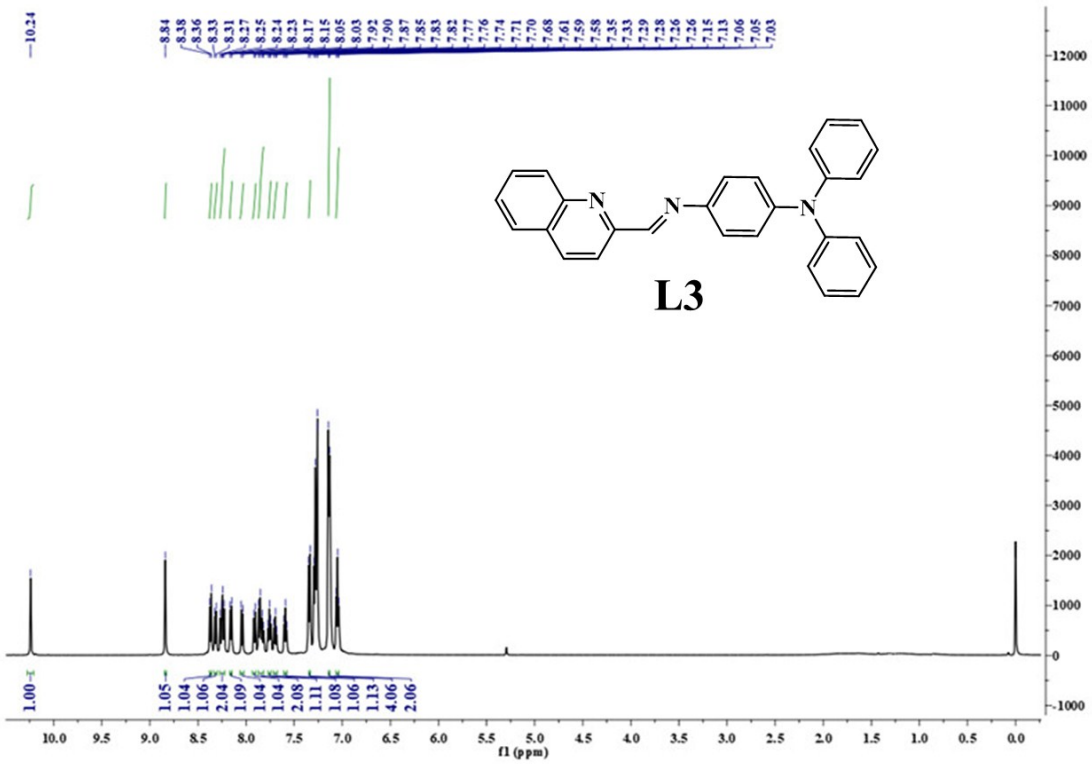

Figure S19. ^{1}H NMR (500 MHz) of **L1-L3**

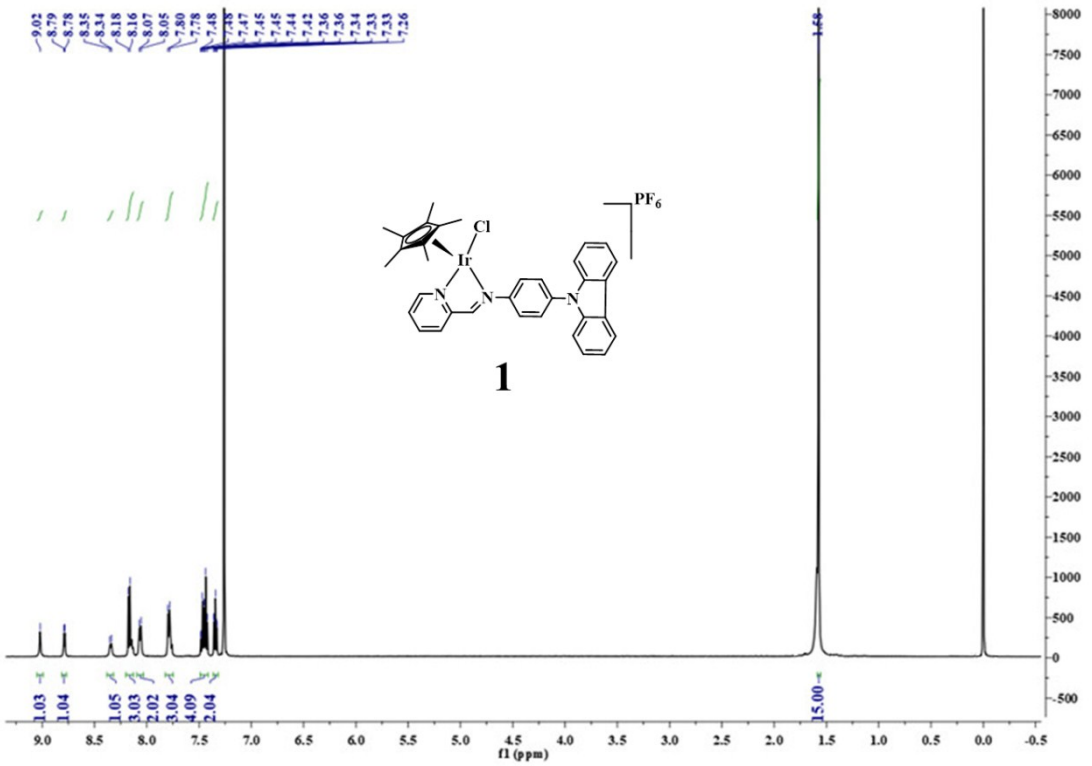

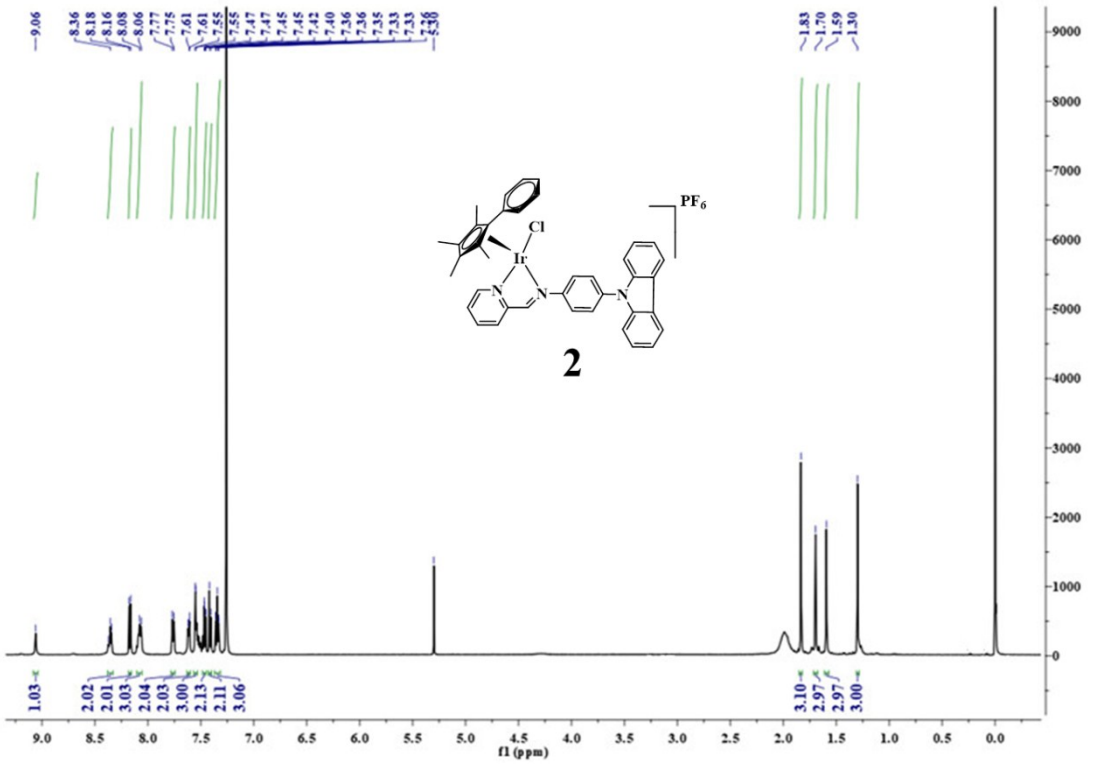
PF6
Cl
Ir
N
N
N
2
f1 (ppm)

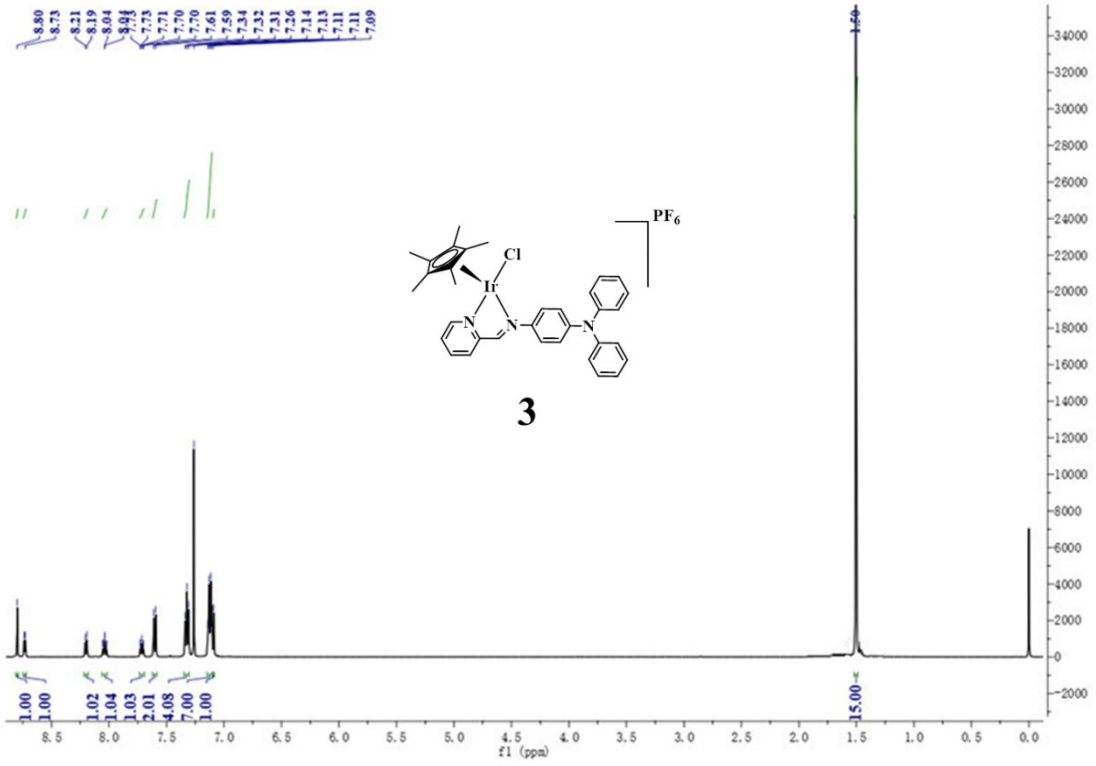
PF6
Cl
Ir
N
N
N
3
f1 (ppm)

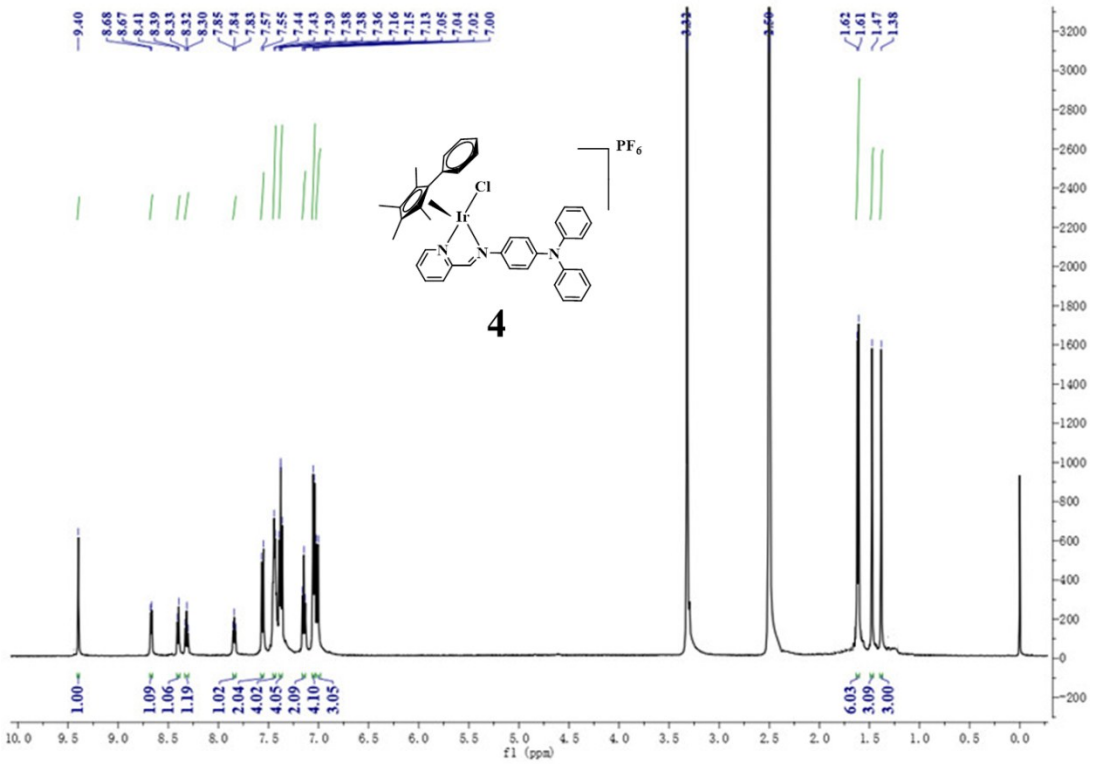
PF6
Cl
Ir
N
N
N
4
fl (ppm)

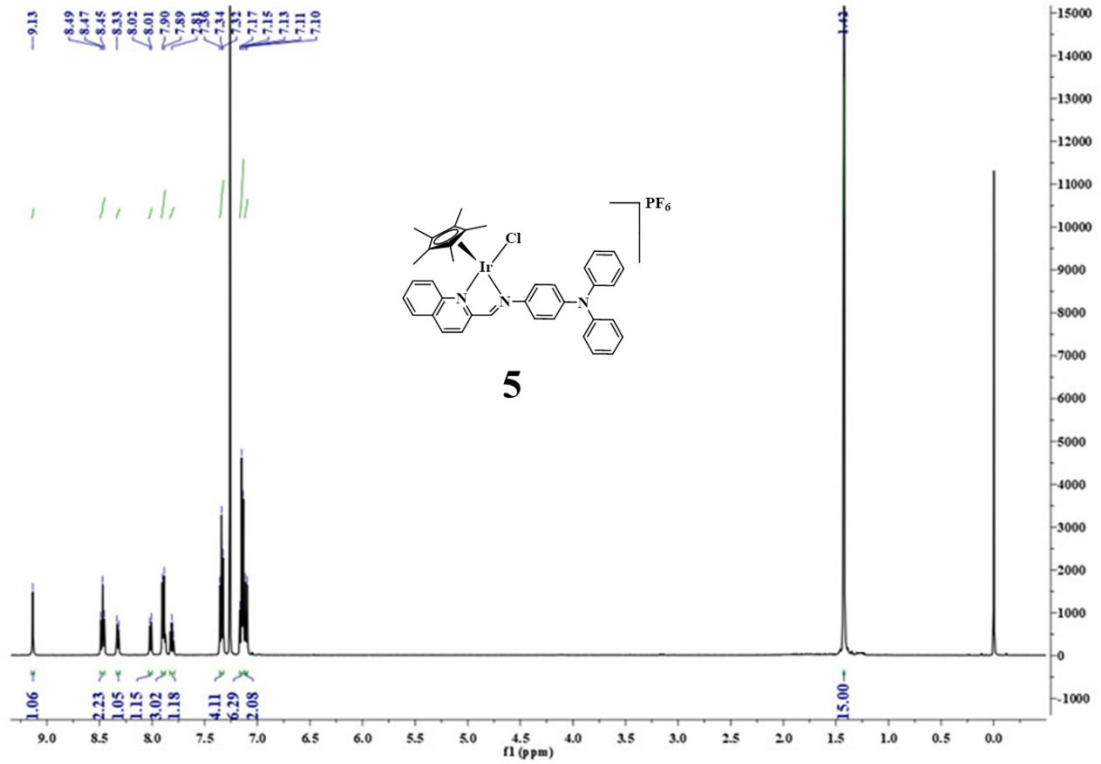
PF6
Cl
Ir
N
N
N
5
fl (ppm)

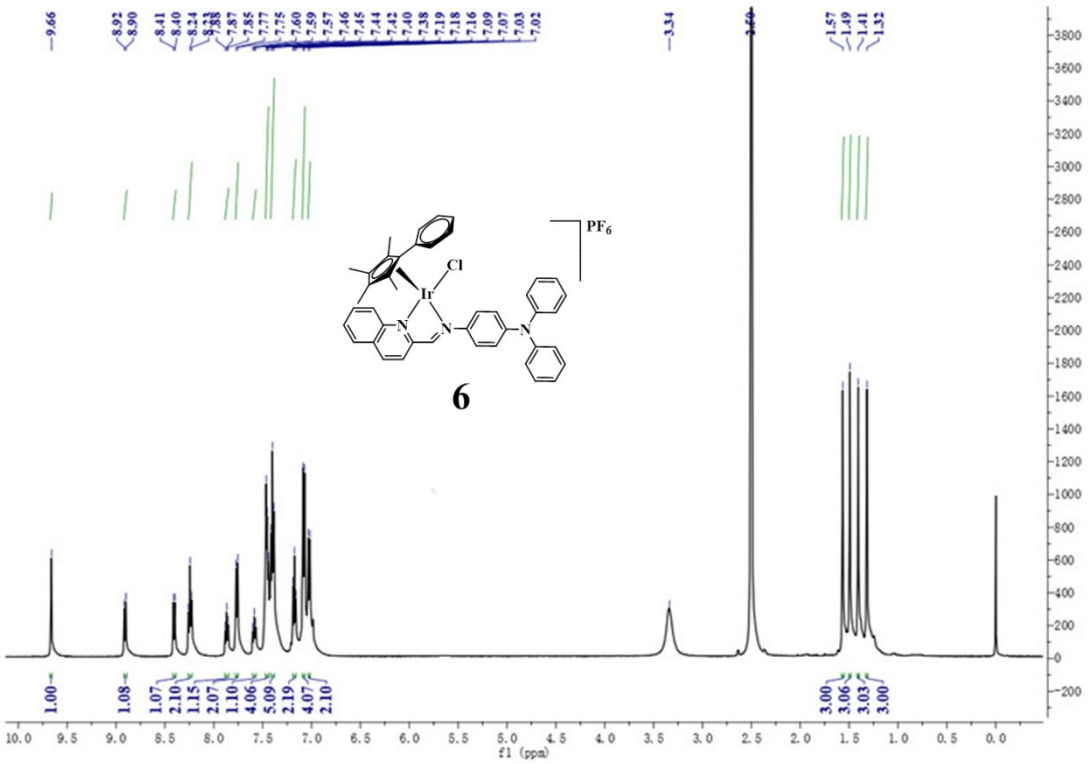
PF6
Cl
Ir
N
N
N
6
f1 (ppm)

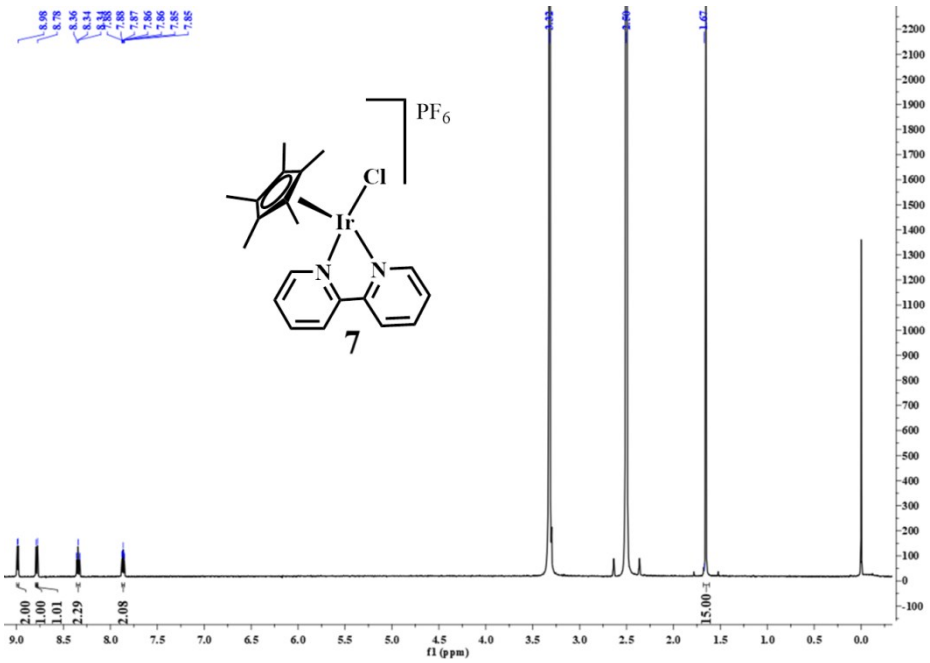
PF6
Cl
Ir
N
N
7
f1 (ppm)

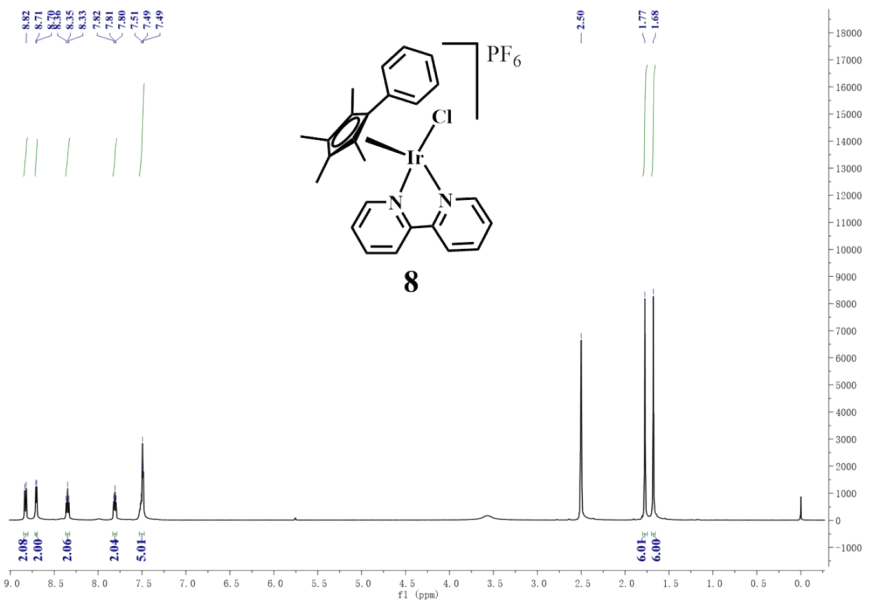

Figure S20. ^{1}H NMR spectra (500 MHz) of **1-8**

^{13}C NMR Spectra

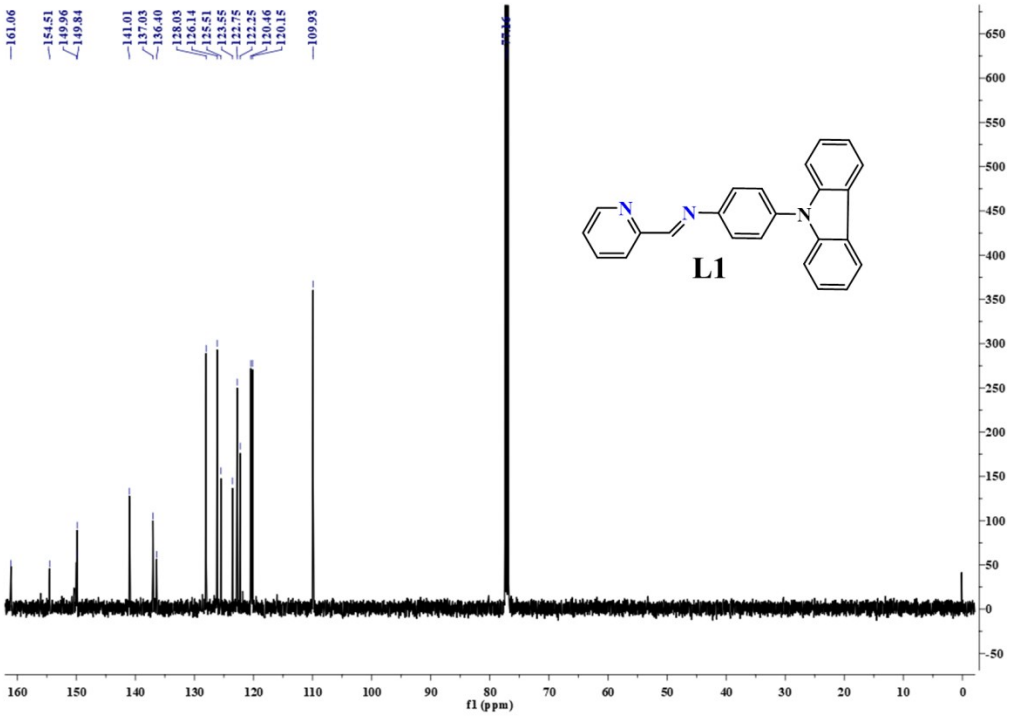

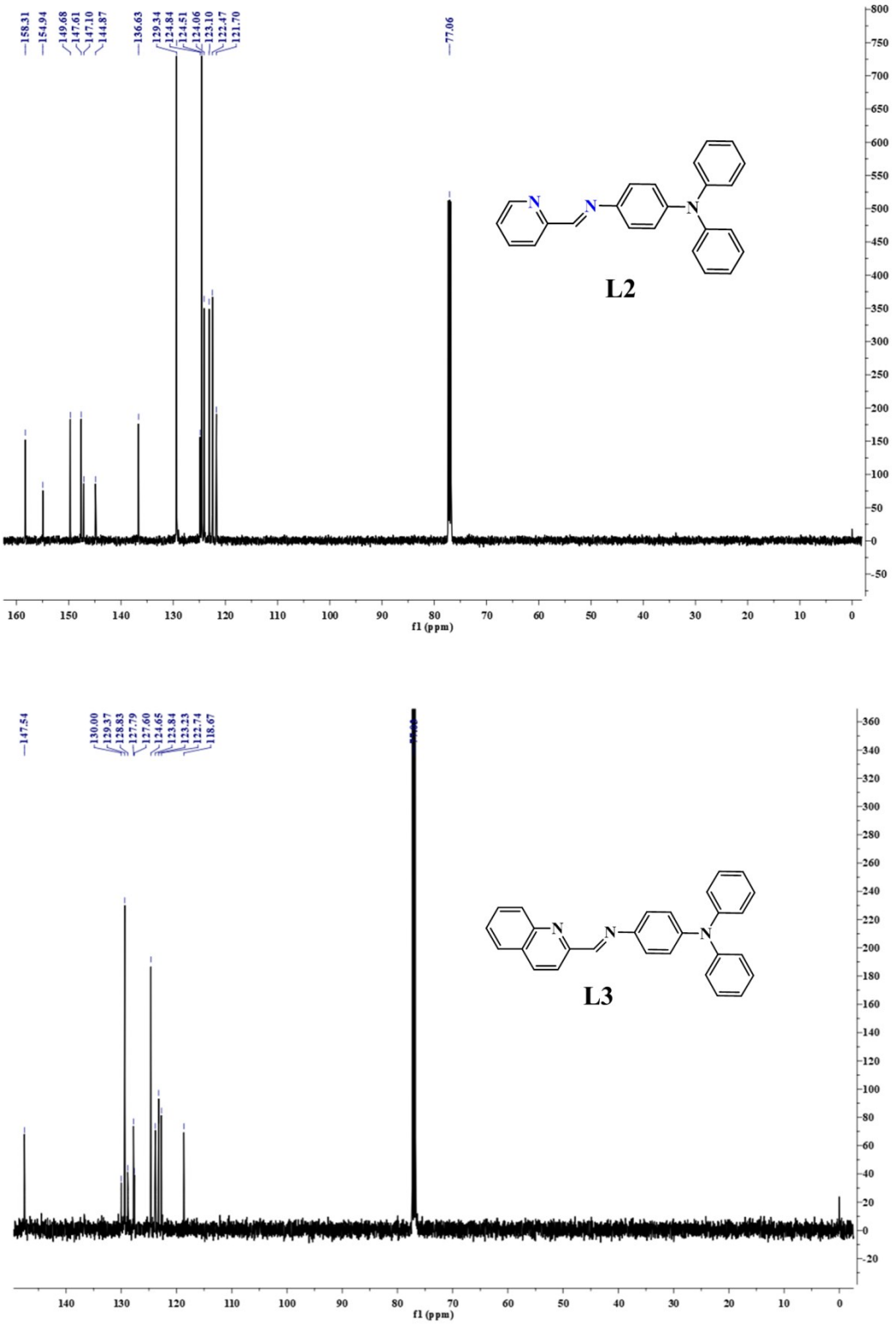

Figure S21. ^{13}C NMR spectra of **L1**-**L3**

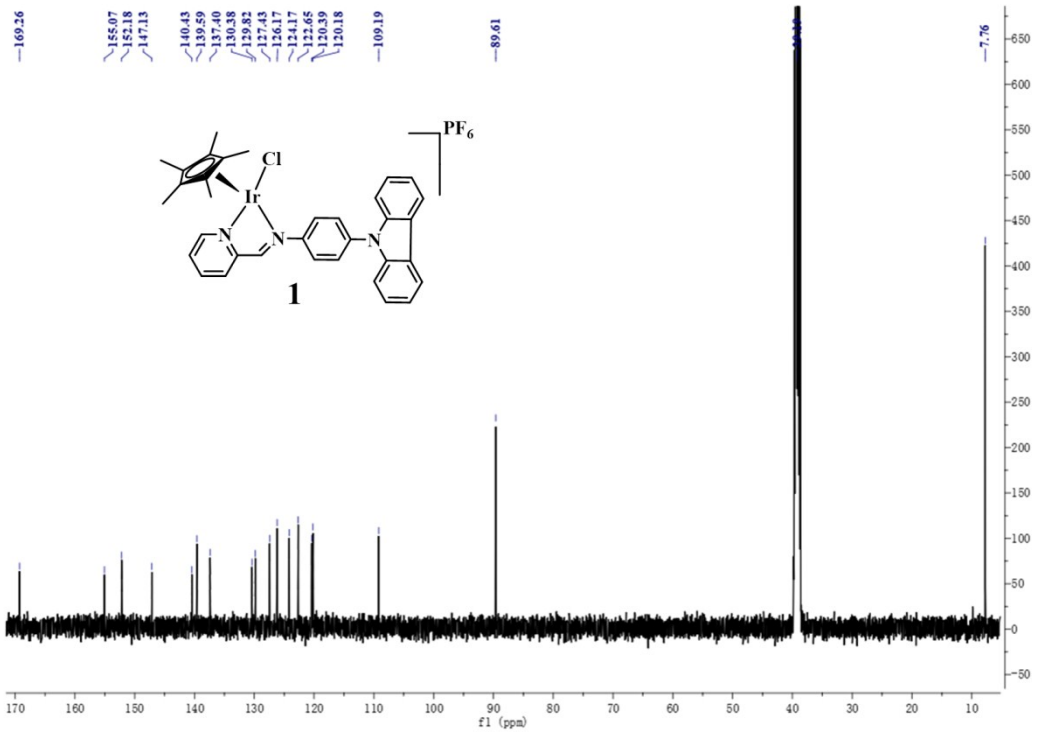
169.26
155.07
152.18
147.13
140.43
139.59
137.40
130.38
129.82
127.43
126.17
124.17
122.65
120.39
120.18
109.19
89.61
39.10
7.76
PF6
Cl
Ir
N
N
N
1
f1 (ppm)

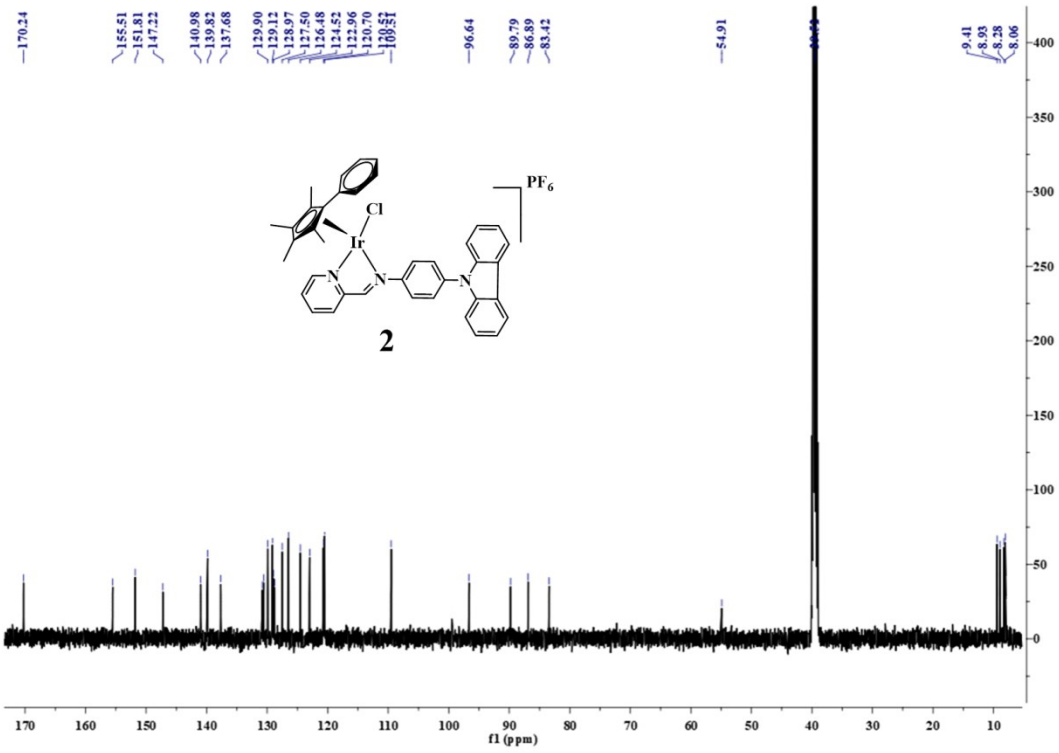
170.24
155.51
151.81
147.22
140.98
139.82
137.68
129.90
129.12
128.97
127.50
126.48
124.52
122.96
120.70
109.51
96.64
89.79
86.89
83.42
54.91
39.10
9.41
8.93
8.28
8.06
PF6
Cl
Ir
N
N
N
2
f1 (ppm)

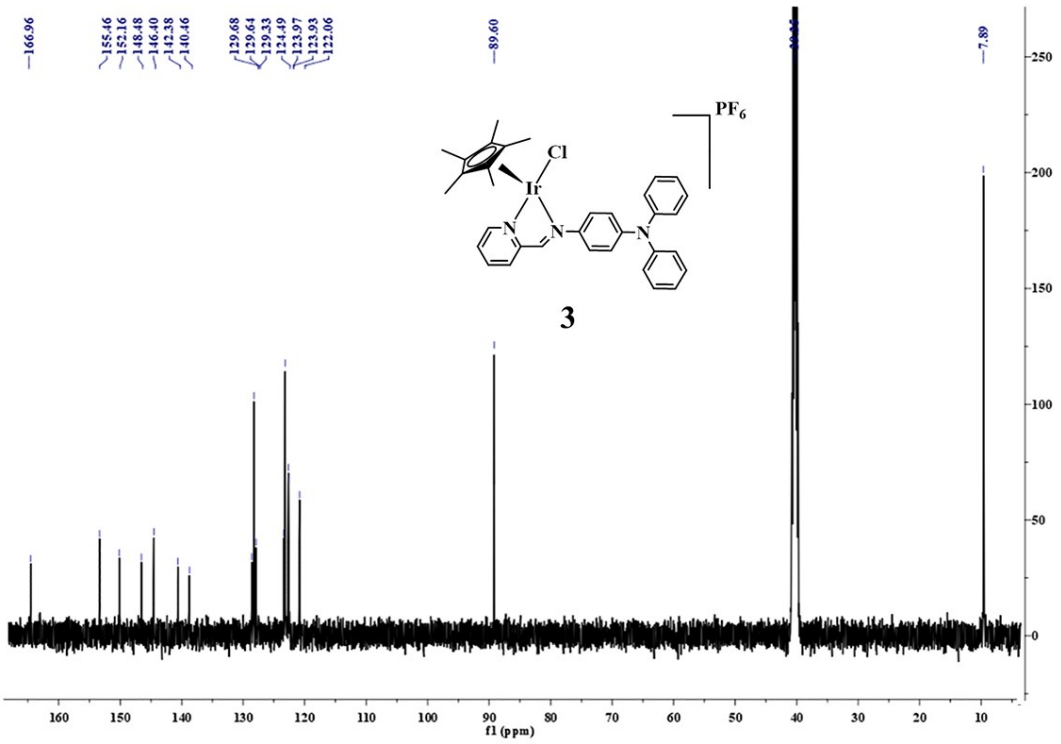
166.96
155.46
152.16
148.48
146.40
142.38
140.46
129.68
129.64
129.33
124.49
123.97
123.93
122.06
89.60
40.00
7.89
PF6
Cl
Ir
N
N
N
3
f1 (ppm)

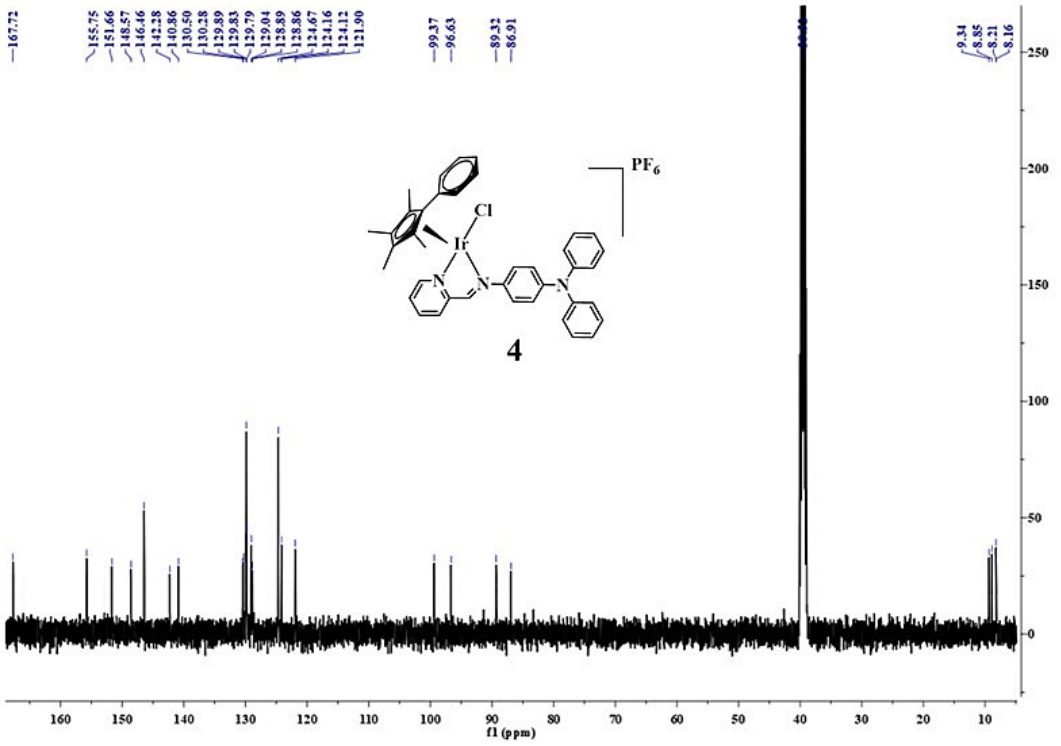
167.72
155.75
151.66
148.57
146.46
142.28
140.86
130.50
130.28
129.89
129.83
129.79
129.04
128.89
128.86
124.67
124.16
124.12
121.90
99.37
96.63
89.32
86.91
40.00
9.34
8.85
8.21
8.16
PF6
Cl
Ir
N
N
N
4
f1 (ppm)

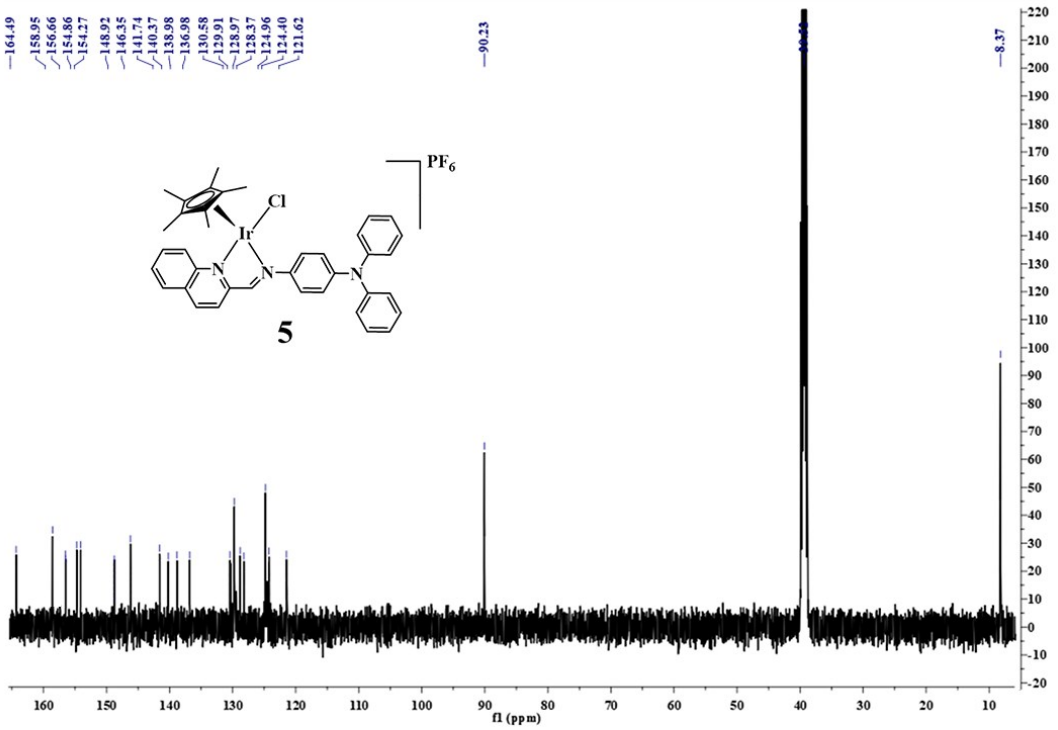
164.49
158.95
156.66
154.86
154.27
148.92
146.35
141.74
140.37
138.98
136.98
130.58
129.91
128.97
128.37
124.96
124.40
121.62
90.23
40.46
8.37
PF6
Cl
Ir
N
N
N
5
f1 (ppm)

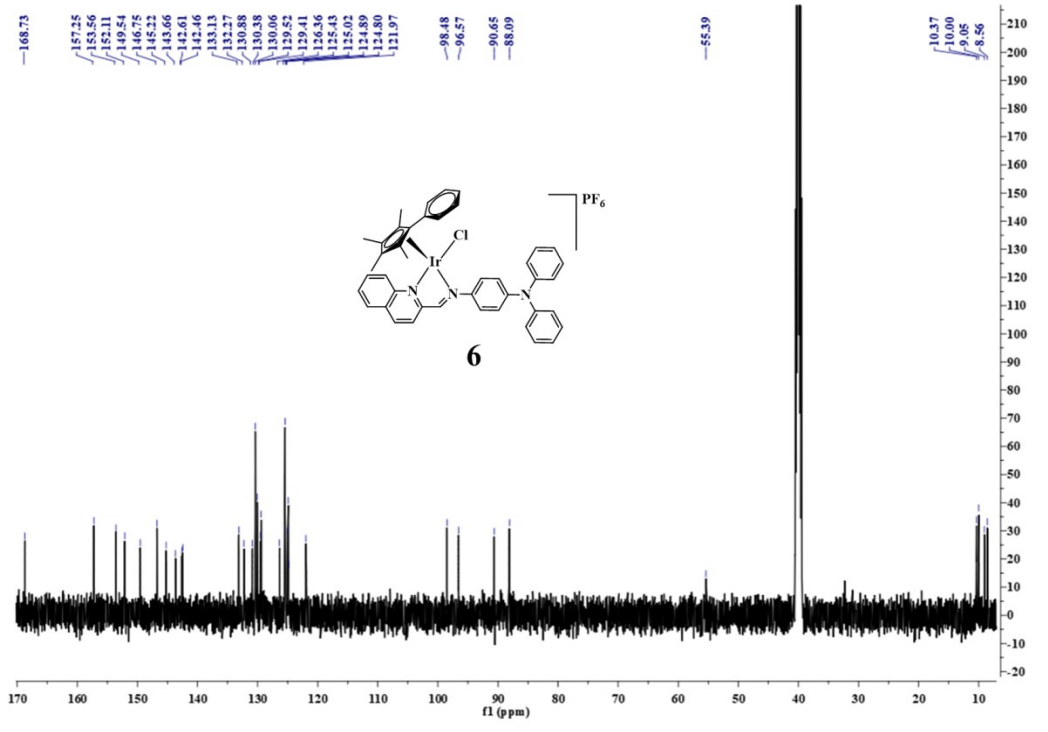
168.73
157.25
153.56
152.11
149.54
146.75
145.22
143.66
142.61
142.46
133.13
132.27
130.88
130.38
130.06
129.52
129.41
126.36
125.43
125.02
124.89
124.80
121.97
98.48
96.57
90.65
88.09
55.39
40.46
10.37
10.00
9.05
8.56
PF6
Cl
Ir
N
N
6
f1 (ppm)

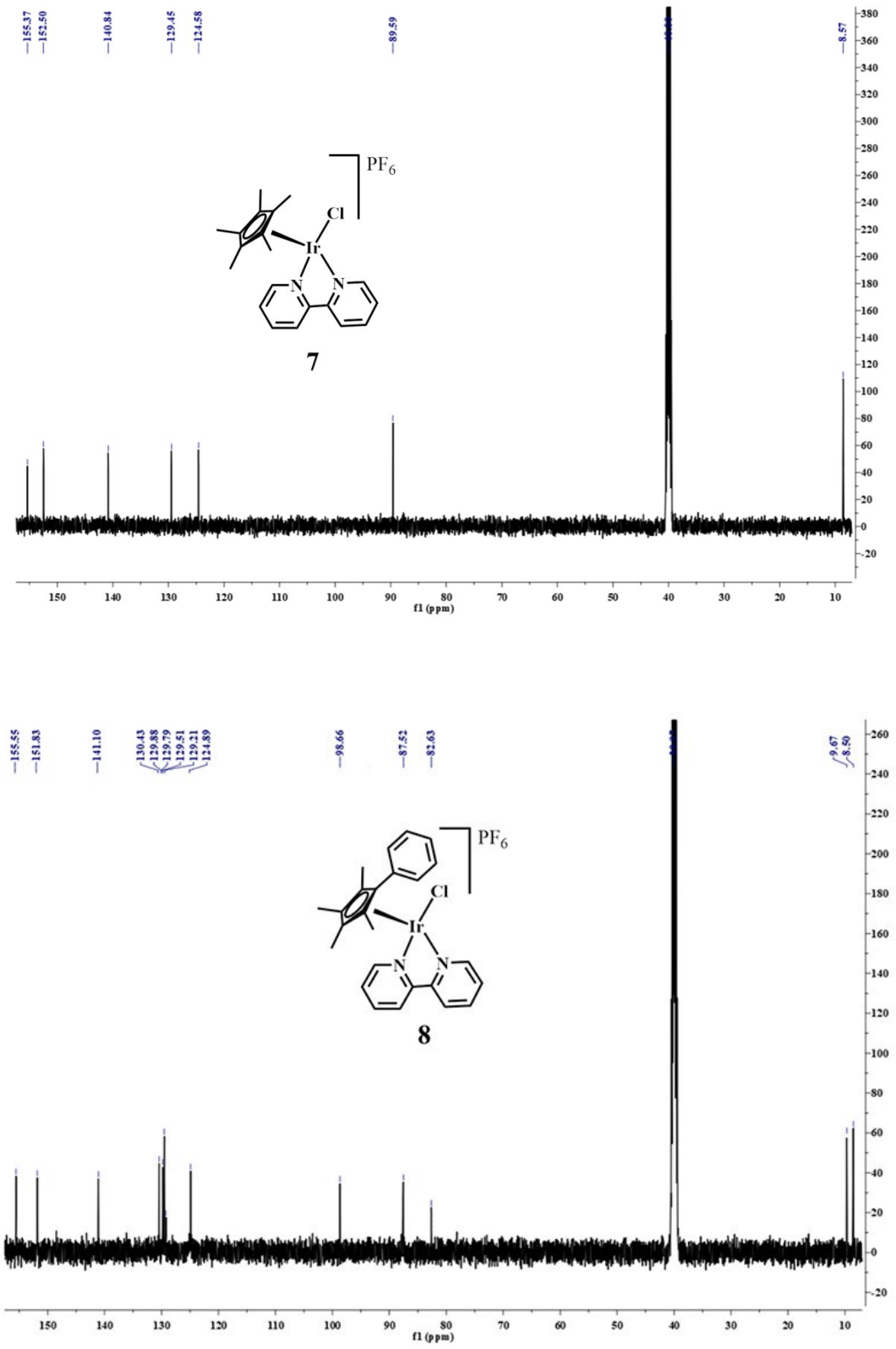

Figure S22. ^{13}C NMR spectra of **1-8**

ESI-MS

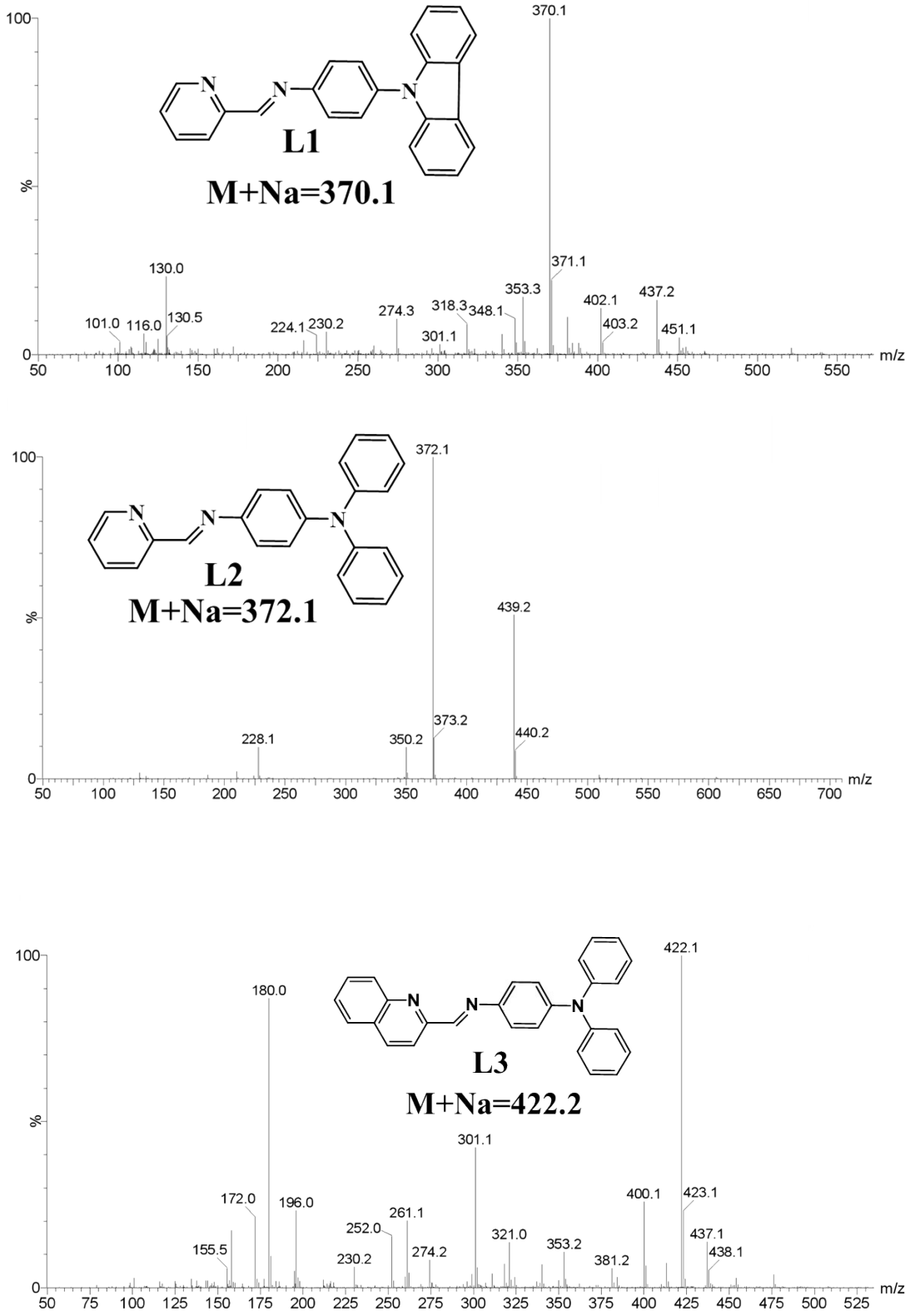

Figure S23. EIS-MS of chelating ligands **L1-L3.**

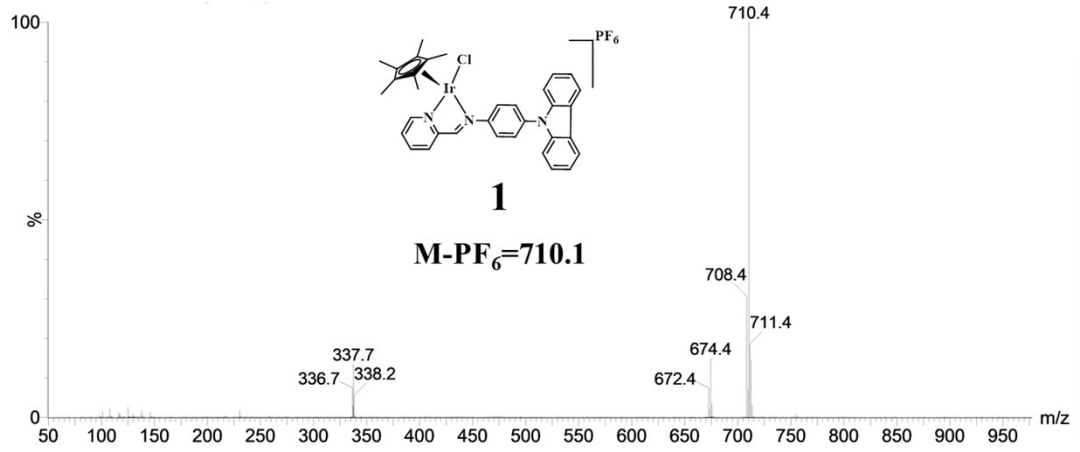
100
%
0
710.4
PF6
Cl
Ir
N
N
N
1
M-PF6=710.1
708.4
711.4
674.4
672.4
337.7
336.7
338.2
50 100 150 200 250 300 350 400 450 500 550 600 650 700 750 800 850 900 950
m/z

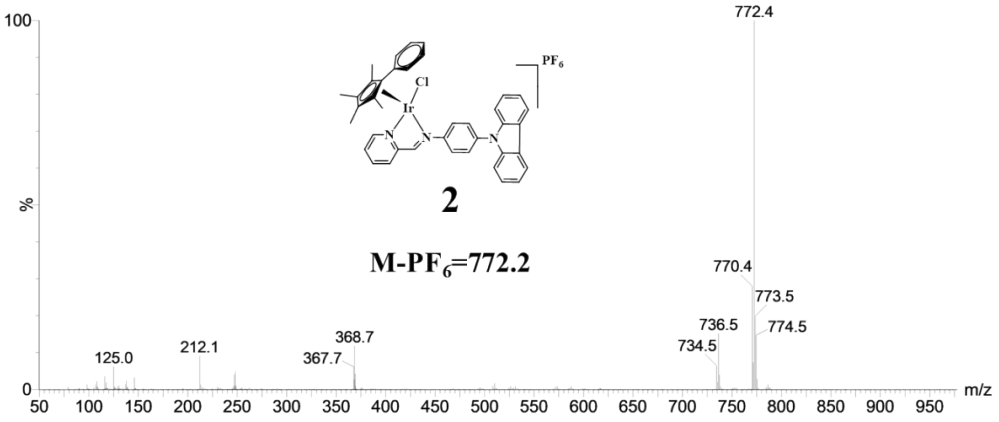
100
%
0
772.4
PF6
Cl
Ir
N
N
N
2
M-PF6=772.2
770.4
773.5
736.5
774.5
734.5
368.7
367.7
212.1
125.0
50 100 150 200 250 300 350 400 450 500 550 600 650 700 750 800 850 900 950
m/z

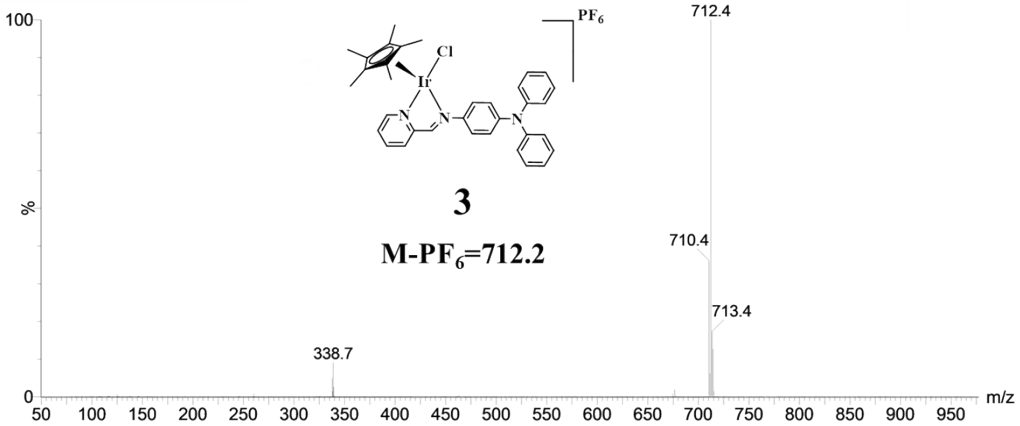
100
%
0
712.4
PF6
Cl
Ir
N
N
N
3
M-PF6=712.2
710.4
713.4
338.7
50 100 150 200 250 300 350 400 450 500 550 600 650 700 750 800 850 900 950
m/z

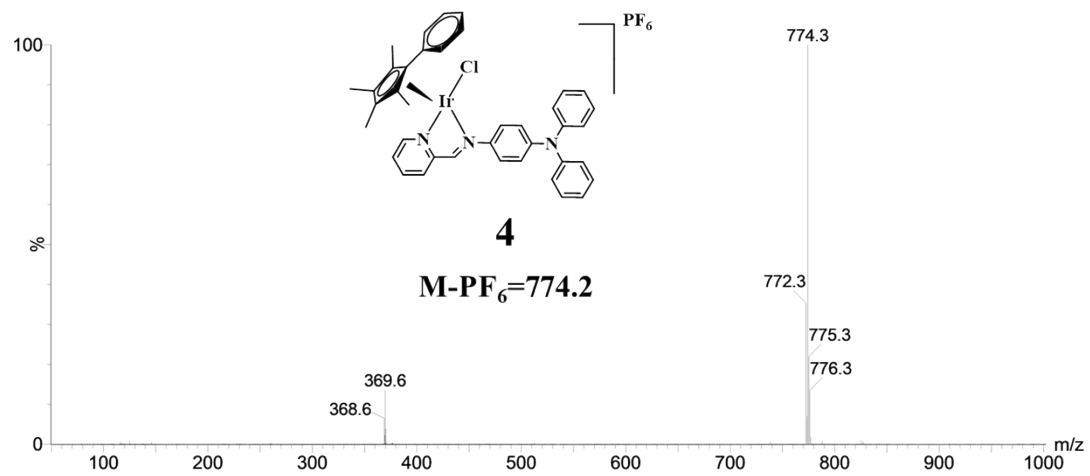
PF6
Cl
Ir
N
N
N
4
M-PF6=774.2
774.3
772.3
775.3
776.3
369.6
368.6
100
%
0
100
200
300
400
500
600
700
800
900
1000
m/z

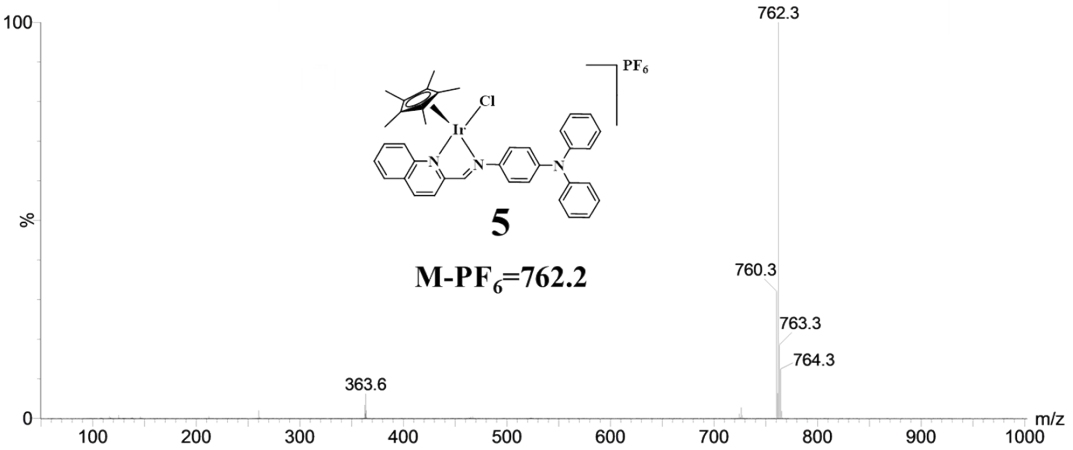
PF6
Cl
Ir
N
N
N
5
M-PF6=762.2
762.3
760.3
763.3
764.3
363.6
100
%
0
100
200
300
400
500
600
700
800
900
1000
m/z

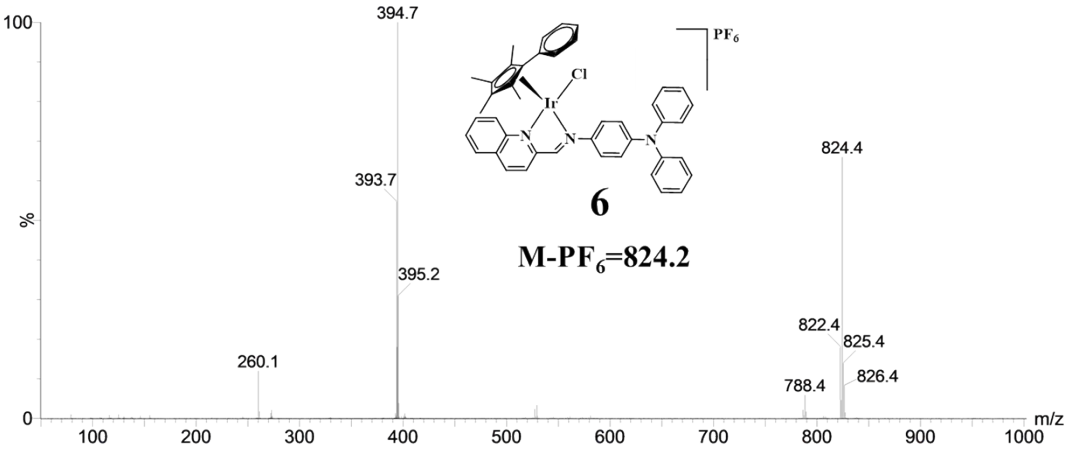
PF6
Cl
Ir
N
N
N
6
M-PF6=824.2
394.7
393.7
395.2
824.4
822.4
825.4
826.4
788.4
260.1
100
%
0
100
200
300
400
500
600
700
800
900
1000
m/z

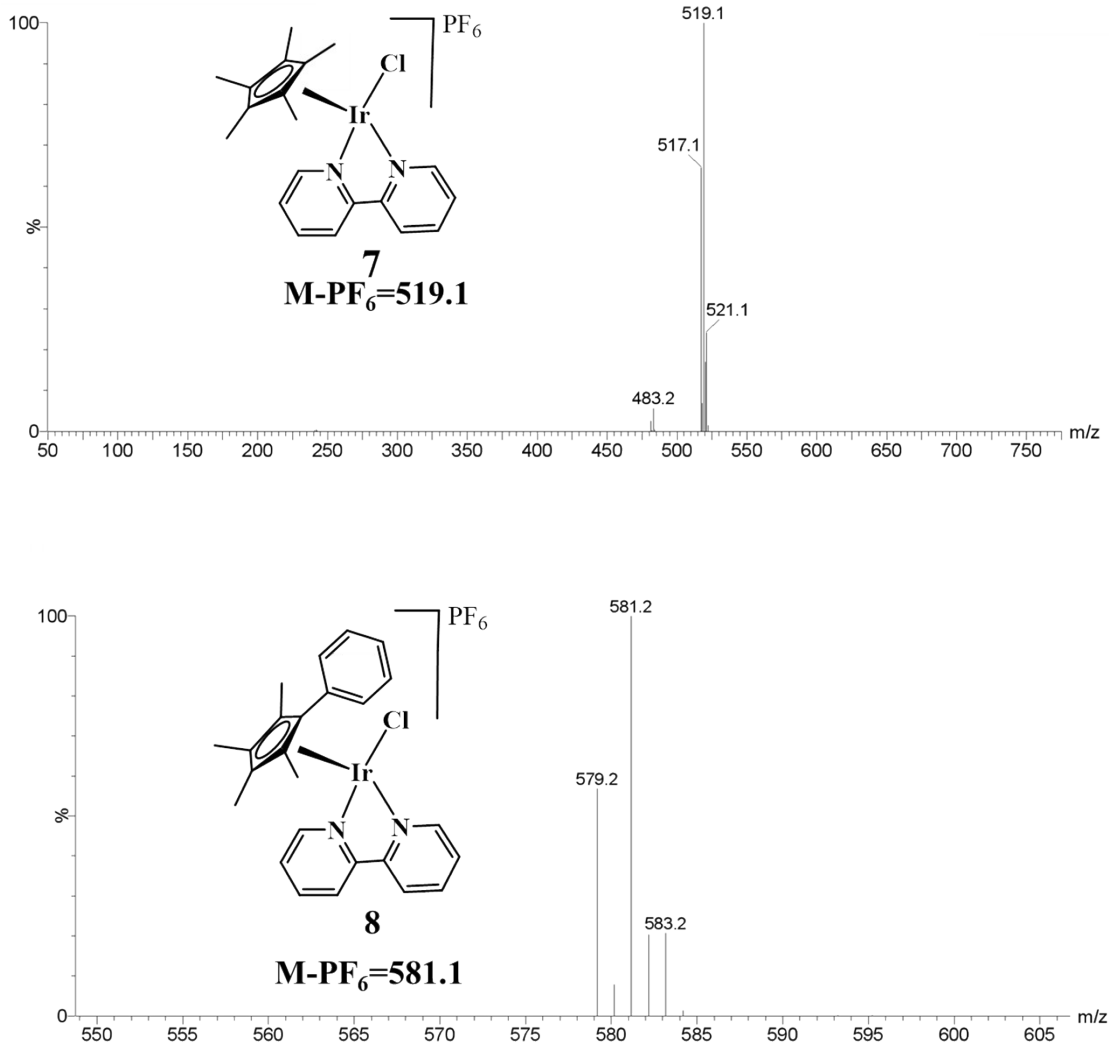

Figure S24. EIS-MS of **1-8.**

Tables

Table S1 Crystallographic data for [(η^5-C_5Me_5)Ir(L1)Cl]PF_6 (**1**)

formula	$C_{34}H_{32}ClF_6\ IrN_3P\cdot 0.5CH_2Cl_2$
MW	897.71
cryst size (mm)	0.43 * 0.30 * 0.19
λ(Å)	0.71073
temp (°C)	25
cryst syst	Orthorhombic
space group	Pcca
a (Å)	27.215(3)
b (Å)	19.8345(17)
c (Å)	12.9815(11)
α (°)	90
β (°)	90
γ (°)	90
vol ($Å^3$)	7007.4(11)
Z	8
density (calc) ($Mg\cdot m^{-3}$)	1.702
abs coeff (mm^{-1})	4.070
F(000)	3528
θ range (deg)	2.40 to 25.02
index ranges	$-32 \le h \le 29$, $-17 \le k \le 23$, $-15 \le l \le 15$
reflns collected	32605
indep reflns	6185 [R(int) = 0.0809]
data / restraints / params	6185 / 0 / 434
final R indices [$I > 2\sigma(I)$]	R1 = 0.0508, wR2 = 0.1259
GOF	1.020
largest diff peak and hole	1.906 and -1.742

Table S2. Flow cytometry analysis to determine the percentages of apoptotic cells, using Annexin V-FITC *vs* PI staining, after exposing A549 cells to **1**.

Compound	Ir concentration	Viable	Population (%)		
			Early apoptosis	Late apoptosis	Non-viable

control		93.32±2.33	0.25±0.03	4.91±0.31	1.52±0.05
	0.25 × IC_{50}	92.62±2.21	1.46±0.05	5.77±0.09	0.15±0.08
	0.5 × IC_{50}	91.57±2.02	0.75±0.09	6.59±0.36	1.09±0.16
1	1.0 × IC_{50}	87.37±1.30	0.36±0.03	7.47±1.01	4.79±0.27
	2.0 × IC_{50}	40.45±1.19	3.08±0.66	25.97±1.09	30.50±1.19
	3.0 × IC_{50}	17.72±0.59	3.87±0.47	31.40±1.89	47.01±1.98

Table S3. Flow cytometry analysis to determine the percentages of apoptotic cells, using Annexin V-FITC *vs* PI staining, after exposing A549 cells to **6**.

Compound	Ir concentration	Viable	Population (%)		
			Early apoptosis	Late apoptosis	Non-viable
control		93.32±2.33	0.25±0.03	4.91±0.31	1.52±0.05
	0.25 × IC_{50}	93.24±2.12	0.96±0.07	5.55±0.19	0.24±0.05
	0.5 × IC_{50}	91.94±2.38	0.50±0.03	5.99±0.37	1.56±0.51
	1.0 × IC_{50}	90.30±1.96	0.24±0.06	7.31±1.30	2.16±0.30
6					
	2.0 × IC_{50}	15.12±1.05	9.50±0.82	65.89±1.86	9.49±1.02
	3.0 × IC_{50}	10.20±0.86	16.25±0.56	67.49±1.63	6.06±0.45

Table S4. The mitochondrial membrane polarization of A549 cells induced by **1**.

Compound	**Ir concentration**	**Population (%)**	
		JC-1 Aggregates	**JC-1 Monomers**
	0. 5 × IC_{50}	88.23±0.32	11.75±0.45
1	1.0 × IC50	82.28±0.23	17.72±0.33
	2.0 × IC50	76.26±0.59	23.71±0.66
Negative Control		91.90±0.96	8.09±0.35
Positive Control		3.17±0.32	96.83±0.89

Table S5. The mitochondrial membrane polarization of A549 cells induced by **6**.

Compound	Ir concentration	Population (%)	
		JC-1 Aggregates	JC-1 Monomers
	0. 5 × IC_{50}	84.31±0.53	15.68±0.85
	1.0 × IC50	81.08±0.20	18.71±0.63
6	2.0 × IC50	53.45±0.69	46.45±0.86
Negative Control		91.90±0.96	8.09±0.35
Positive Control		3.17±0.32	96.83±0.89

Table S6. Cell cycle analysis carried out by flow cytometry using PI staining after exposing A549 cells to **1**.

Compound	Ir concentration	Population (%)		
		G_0/G_1 phase	S phase	G_2/M phase
Control		56.44±1.95	32.72±1.03	9.43±0.12
	0.25 × IC_{50}	56.96±1.90	31.70±2.01	9.71±0.18
	0.5× IC_{50}	52.02±1.06	34.70±2.80	11.54±0.19
1				
	1.0× IC_{50}	49.41±1.43	35.95±1.15	13.10±0.25
	2.0× IC_{50}	49.33±1.53	30.27±1.53	19.44±0.35

Table S7. Cell cycle analysis carried out by flow cytometry using PI staining after exposing A549 cells to **6**.

Compound	Ir concentration	Population (%)		
		G_0/G_1 phase	S phase	G_2/M phase
Control		48.75±0.99	37.56±1.44	11.65±0.15
	0.25 × IC_{50}	52.73±1.30	32.41±2.05	13.10±0.05
	0.5× IC_{50}	55.80±1.18	32.22±2.30	10.40±0.17
6				
	1.0× IC_{50}	58.33±1.36	29.78±1.65	10.70±0.63
	2.0× IC_{50}	65.71±1.03	22.41±1.58	28.64±0.50